INVITED REVIEW

A guide to photosynthetic gas exchange measurements: Fundamental principles, best practice and potential pitfalls

Florian A. Busch[1,2] | Elizabeth A. Ainsworth[3] | Anna Amtmann[4] | Amanda P. Cavanagh[5,6] | Steven M. Driever[7] | John N. Ferguson[5] | Johannes Kromdijk[6,8] | Tracy Lawson[5] | Andrew D. B. Leakey[9] | Jack S. A. Matthews[5] | Katherine Meacham-Hensold[6] | Richard L. Vath[8,10] | Silvere Vialet-Chabrand[11] | Berkley J. Walker[12,13] | Maria Papanatsiou[4]

[1]School of Biosciences and Birmingham Institute of Forest Research, University of Birmingham, Birmingham, UK

[2]Research School of Biology, The Australian National University, Canberra, Australian Captial Territory, Australia

[3]USDA ARS Global Change and Photosynthesis Research Unit, Urbana, Illinois, USA

[4]School of Molecular Biosciences, College of Medical, Veterinary & Life Sciences, University of Glasgow, Glasgow, UK

[5]School of Life Sciences, University of Essex, Colchester, UK

[6]Carl R. Woese Institute for Genomic Biology, University of Illinois, Urbana, Illinois, USA

[7]Centre for Crop Systems Analysis, Wageningen University & Research, Wageningen, The Netherlands

[8]Department of Plant Sciences, University of Cambridge, Cambridge, UK

[9]Departments of Plant Biology and Crop Sciences, University of Illinois Urbana Champaign, Urbana, Illinois, USA

[10]LI-COR Environmental, Lincoln, Nebraska, USA

[11]Department of Plant Sciences, Horticulture and Product Physiology, Wageningen, The Netherlands

[12]Plant Research Laboratory, Michigan State University, East Lansing, Michigan, USA

[13]Department of Plant Biology, Michigan State University, East Lansing, Michigan, USA

Correspondence

Maria Papanatsiou, School of Molecular Biosciences, College of Medical, Veterinary & Life Sciences, University of Glasgow, Glasgow G12 8QQ, UK.
Email: Maria.Papanatsiou@glasgow.ac.uk

Florian A. Busch, School of Biosciences and Birmingham Institute of Forest Research, University of Birmingham, Edgbaston, Birmingham B15 2TT, UK.
Email: f.a.busch@bham.ac.uk

Abstract

Gas exchange measurements enable mechanistic insights into the processes that underpin carbon and water fluxes in plant leaves which in turn inform understanding of related processes at a range of scales from individual cells to entire ecosytems. Given the importance of photosynthesis for the global climate discussion it is important to (a) foster a basic understanding of the fundamental principles underpinning the experimental methods used by the broad community, and (b) ensure best practice and correct data interpretation within the research community. In this review, we outline the biochemical and biophysical parameters of photosynthesis that can be investigated with gas exchange measurements and we provide step-by-step guidance on how to reliably measure them. We advise on best practices for using gas exchange equipment and highlight potential pitfalls in experimental design and data interpretation. The Supporting Information contains

exemplary data sets, experimental protocols and data-modelling routines. This review is a community effort to equip both the experimental researcher and the data modeller with a solid understanding of the theoretical basis of gas-exchange measurements, the rationale behind different experimental protocols and the approaches to data interpretation.

KEYWORDS
carbon reactions, photosynthesis, stomata

1 | INTRODUCTION

For decades, gas exchange techniques using infrared gas analysers (IRGAs) have been widely used to measure fluxes of CO_2 and H_2O into and out of leaves and, less frequently, nonfoliar tissues. These measurements allow for assessments of the physiological performance of leaves and to benchmark the biochemical capacity for photosynthesis (von Caemmerer, 2013; Long & Bernacchi, 2003; Long et al., 1996). Measurements of leaf-level gas exchange enable mechanistic understanding of the molecular processes determining carbon and water fluxes and inform understanding of ecosystem function (Bernacchi et al., 2013; Ely et al., 2021; Rogers et al., 2017). Built on a long history of technology innovation in the space of chamber design and analyser setup (Bloom et al., 1980; Gaastra, 1959; Long & Hallgren, 1985), current commercial gas exchange systems are precise, often portable, and relatively easy to use. They have enabled measurements of in situ photosynthetic CO_2 assimilation (A) and stomatal conductance (g_s) in diverse ecosystems from the tropics (e.g., Carter et al., 2021; Slot & Winter, 2017) to the arctic (Rogers et al., 2019), and from grasslands to forests to agricultural fields (e.g., Coast et al., 2021; Dillaway & Kruger, 2010; Koester et al., 2016; Wohlfahrt et al., 1999).

Gas exchange measurements can test how fluxes of CO_2 and H_2O between the leaf and the atmosphere change as environmental conditions in the leaf chamber are manipulated (e.g., Ball et al., 1987; Leakey et al., 2006; Li et al., 2021; Miner et al., 2017; Wolz et al., 2017) and how long-term growth under different environmental conditions impacts rates, biochemical capacity and diffusional limitations of photosynthesis (see Ainsworth & Long, 2005; Medlyn et al., 2002; Wittig et al., 2007; Yan et al., 2016 for meta-analyses). Gas exchange measurements have also improved our understanding of the physiology of species operating different types of photosynthesis (such as C_3, C_4, CAM) (Hogewoning et al., 2021; Lundgren et al., 2016; Sage & Kubien, 2007; Schuster & Monson, 1990).

Several introductory guides to gas exchange have been published, mostly focusing on the details of a particular measurement technique (Busch, 2018; Evans & Santiago, 2014; Haworth et al., 2018; Long & Bernacchi, 2003; Parsons et al., 1997). In the following, we give an overview of the biochemical and biophysical photosynthetic processes that can be investigated with gas

exchange measurements and outline the parameters that can be estimated. We then discuss suitable approaches for quantifying these parameters with photosynthetic gas exchange techniques in C_3 plants, which operate the dominant photosynthetic pathway. However, in many cases the approaches can be applied to C_4 or CAM species with appropriate modifications, some of which are discussed in this article.

While recording gas exchange data with current commercially available equipment is relatively easy, the obtained data are not necessarily meaningful. Both the correct experimental design and the correct data interpretation are crucial for obtaining high quality information. We therefore include here "how-to" tips that have not been part of prior guides. Of course, the specific design of commercial gas exchange equipment varies between manufacturers and the reader should refer to the manufacturer manuals for their operation (see, e.g., LI-COR, 2012, 2022; Walz, 2019). Our recommendations and nomenclature are based on current common practice but deviate where we feel a new approach is beneficial. In particular, this includes new recommendations for fitting light response curves. The review will thus equip the novice with a solid foundation in the technique and also offers the experienced researcher some new ideas. Overall, our intention is to outline procedures that facilitate successful measurements, but we note that these recommendations can and may have to be modified to address specific research questions.

2 | KEY PARAMETERS OBTAINED FROM GAS EXCHANGE MEASUREMENTS

Photosynthetic CO_2 fixation is the result of a complex set of biochemical and biophysical processes, many of which can be probed with gas exchange techniques. Gas exchange measurements inform us about diverse aspects of carbon and water relations, ranging from processes associated with the light-dependent and light-independent reactions to CO_2/H_2O diffusion and the sink capacity of a leaf. The only information that gas exchange measurements give us directly are concentrations of CO_2 and H_2O and the associated net fluxes. However, a wide range of parameters can be estimated from these values indirectly, based on certain assumptions. These parameters
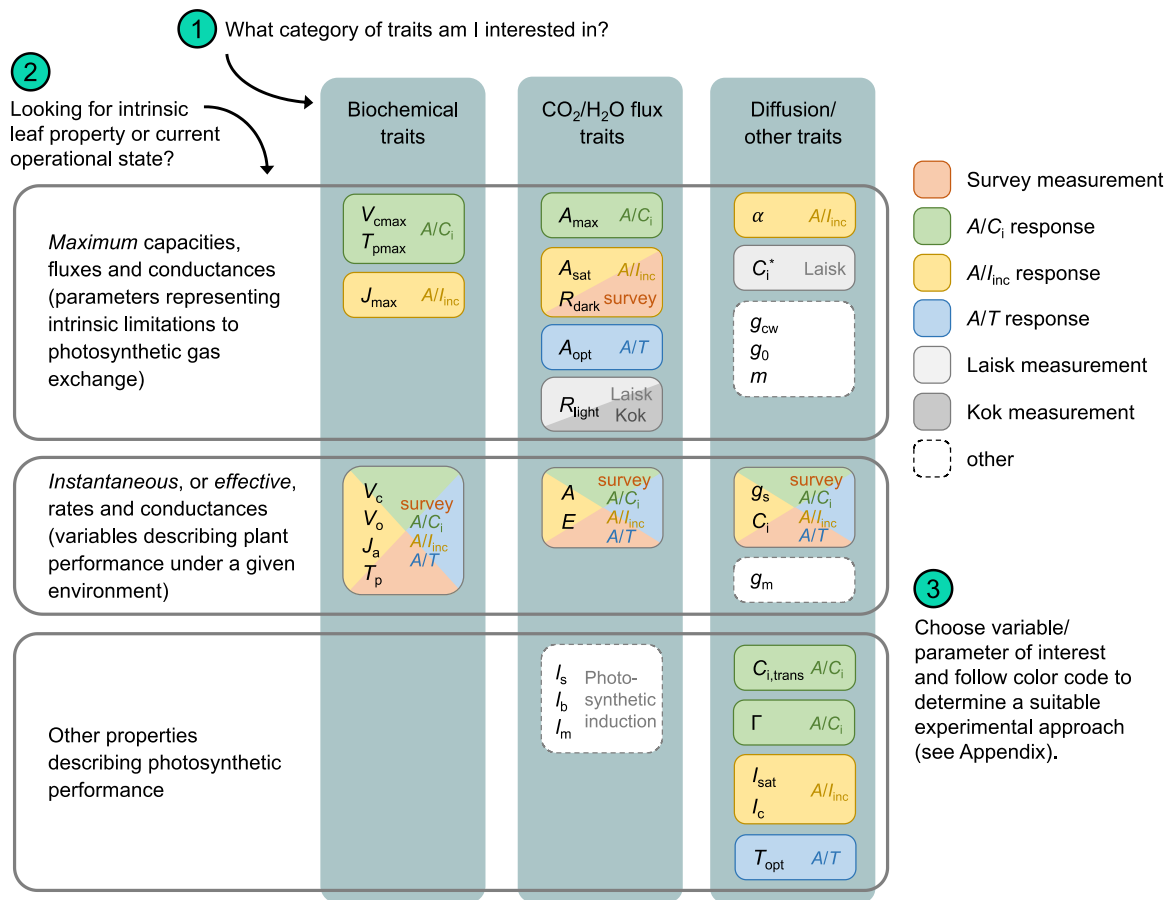
FIGURE 1   Choosing the right parameters to measure for the research question at hand. Photosynthetic properties can be separated into traits describing biochemical and gas diffusion properties as well as gas fluxes into or out of the leaf. The first step is therefore to determine the broad category of traits the gas exchange measurements to assess. The next question is whether the photosynthetic properties of interest relate to an instrinsic leaf property or the operational state of a leaf under a specific environmental condition. Other, more descriptive, properties can also be estimated from gas exchange measurements. The parameters that can then be quantified in support of the research question are given along with suitable experimental approaches for each, described in detail in Supporting Information S1. Definitions for the parameters and variables can be found in Table 1.

can be crudely divided into three categories (Figure 1, Table 1): The first category informs on the 'maximum' capacities of the leaf, and its parameters describe the intrinsic properties of a leaf's investment into different photosynthetic aspects. These parameters may have a fixed temperature response or may change throughout leaf development but can otherwise be treated as constants. The second category informs on the current physiological state of a leaf, that is, the 'instantaneous' or 'effective' rates that are realised during the instance of the measurement. These are variables that can be expected to change in the short-term (seconds to hours) with changing environmental conditions, such as light intensity, atmospheric [CO_2] or water status. The third category includes parameters that describe some aspect of photosynthetic performance, but may not directly correspond to a single identifiable physiological trait. Examples include the CO_2 concentration at which A transitions from one biochemical limitation to another, or the relative contribution of different physiological processes limiting A. For a list and definitions of all parameters see Table 1.

2.1 | Maximum capacity, flux and conductance

The *maximum capacity* of the biochemical processes is captured by three variables: (i) The maximum rate of ribulose 1,5-bisphosphate (RuBP) carboxylation (V_{cmax}) represents the capacity of RuBP consumption in the Calvin–Benson–Bassham (CBB) cycle, with ribulose-bisphosphate carboxylase-oxygenase (Rubisco) thought to be the key rate-limiting step. (ii) The maximum rate of photosynthetic electron transport (J_{max}) represents all processes involved in RuBP regeneration, and it is thought to be limited by the rate of water splitting at photosystem II (PSII) and/or the rate of electron transport through cytochrome b_6f (Johnson & Berry, 2021). V_{cmax} and J_{max} are the rates that can theoretically be achieved when the chloroplastic CO_2 concentration (or light intensity in case of J_{max}) is infinite, and no process other than Rubisco carboxylation (or electron transport) is limiting. (iii) The maximum rate of triose phosphate utilisation, T_{pmax}, relates to the capacity of starch synthesis or sucrose export from the chloroplast. T_{pmax} may reflect a limitation of other plant organs to metabolise or store the new assimilates and is thus

TABLE 1 Variables, units and typical values under ambient conditions.

Variable		Unit with scaling	Typical value at 25°C [a]
A	Net CO_2 assimilation rate	$\mu mol\ m^{-2}\ s^{-1}$	10–20
A_c	Potential Rubisco-limited net CO_2 assimilation rate	$\mu mol\ m^{-2}\ s^{-1}$	
A_j	Potential electron transport-limited net CO_2 assimilation rate	$\mu mol\ m^{-2}\ s^{-1}$	
A_{max}	Maximum CO_2 assimilation rate at light and CO_2 saturated conditions	$\mu mol\ m^{-2}\ s^{-1}$	20–40
A_{opt}	CO_2 assimilation rate at the photosynthetic temperature optimum	$\mu mol\ m^{-2}\ s^{-1}$	10–30
A_p	Potential triose phosphate utilisation-limited net CO_2 assimilation rate	$\mu mol\ m^{-2}\ s^{-1}$	
A_{sat}	Light saturated CO_2 assimilation rate at ambient C_a	$\mu mol\ m^{-2}\ s^{-1}$	10–20
C_a	Ambient (atmospheric) CO_2 mole fraction	$\mu mol\ CO_2\ mol^{-1}$ air	420
C_c	Chloroplastic CO_2 mole fraction	$\mu mol\ CO_2\ mol^{-1}$ air	200
C_i	Intercellular CO_2 mole fraction	$\mu mol\ CO_2\ mol^{-1}$ air	300
$C_{i,trans}$	Intercellular CO_2 mole fraction, at which A transitions from RuBP-saturated to RuBP-limited	$\mu mol\ CO_2\ mol^{-1}$ air	350
C_i^*	Intercellular CO_2 compensation point in the absence of respiration	$\mu mol\ CO_2\ mol^{-1}$ air	45
E	Transpiration rate	$mmol\ m^{-2}\ s^{-1}$	5
g_0	'Residual' stomatal conductance of BB model	$mol\ m^{-2}\ s^{-1}$	0.05
g_{bc}	Boundary layer conductance to CO_2	$mol\ m^{-2}\ s^{-1}$	1–2.5
g_{bw}	Boundary layer conductance to H_2O vapour, $=1.37\ g_{bc}$	$mol\ m^{-2}\ s^{-1}$	1.5–3.5
g_{cw}	Cuticular conductance to H_2O vapour	$mol\ m^{-2}\ s^{-1}$	0.05
g_{sc}	Stomatal conductance to CO_2	$mol\ m^{-2}\ s^{-1}$	0.25
g_{sw}	Stomatal conductance to H_2O vapour, $=1.6\ g_{sc}$	$mol\ m^{-2}\ s^{-1}$	0.4
g_m	Mesophyll conductance to CO_2	$mol\ m^{-2}\ s^{-1}$	0.3
I_c	Light compensation point	$\mu mol\ m^{-2}\ s^{-1}$	15
I_{inc}	Flux density of incident photosynthetically active radiation	$\mu mol\ m^{-2}\ s^{-1}$	0–2000
I_{sat}	Saturating light intensity	$\mu mol\ m^{-2}\ s^{-1}$	500
J	Potential rate of electron transport at a given light intensity	$\mu mol\ m^{-2}\ s^{-1}$	100
J_a	Actual rate of electron transport	$\mu mol\ m^{-2}\ s^{-1}$	0–150
J_{max}	Maximum rate of electron transport	$\mu mol\ m^{-2}\ s^{-1}$	200
K_c	Michaelis–Menten constant for CO_2	$\mu mol\ mol^{-1}$ [b]	250–900
		μM	8–30
K_o	Michaelis–Menten constant for O_2	$mmol\ mol^{-1}$ [b]	200–500
		μM	250–650
l_b	Relative biochemical limitation	Dimensionless	
l_m	Relative mesophyll limitation	Dimensionless	
l_s	Relative stomatal limitation	Dimensionless	
m	Empirical slope of BB model	Dimensionless	
O	Oxygen mole fraction	$mmol\ O_2\ mol^{-1}$ air	210
P	Atmospheric pressure	kPa	100
R_d	Rate of respiratory CO_2 release from the mitochondria (assumed here to be independent of irradiance)	$\mu mol\ m^{-2}\ s^{-1}$	1

TABLE 1 (Continued)

Variable		Unit with scaling	Typical value at 25°C [a]
R_{dark}	Apparent rate of respiration at the leaf level in the dark	µmol m^{-2} s^{-1}	1
R_{light}	Apparent rate of respiration at the leaf level in the light	µmol m^{-2} s^{-1}	0.7
RH	Relative humidity (as a fraction)	Dimensionless	0.3–0.8
$S_{c/o}$	Relative specificity of Rubisco	kPa kPa^{-1} [b]	1900–2900
		M M^{-1}	70–110
s_c	Henry's law solubility constant for CO_2	M kPa^{-1}	0.000334
s_o	Henry's law solubility constant for O_2	M kPa^{-1}	0.0000132
T_{leaf}	Leaf temperature	°C	25
T_{opt}	Photosynthetic temperature optimum	°C	20–35
T_p	Actual rate of triose phosphate utilisation	µmol m^{-2} s^{-1}	0–15
T_{pmax}	Maximum rate of triose phosphate utilisation	µmol m^{-2} s^{-1}	5–15
V_c	Actual rate of RuBP carboxylation	µmol m^{-2} s^{-1}	0–40
V_{cmax}	Maximum rate of carboxylation by Rubisco	µmol m^{-2} s^{-1}	50–150
V_o	Actual rate of RuBP oxygenation	µmol m^{-2} s^{-1}	0–15
V_{omax}	Maximum rate of RuBP oxygenation	µmol m^{-2} s^{-1}	20–60
VPD_{leaf}	Leaf-to-air vapour pressure difference	kPa	0.5–3
w_a	Water vapour mole fraction in the atmosphere	mmol H_2O mol^{-1} air	
w_i	Water vapour mole fraction within the leaf	mmol H_2O mol^{-1} air	
W_c	Rubisco-limited rate of carboxylation	µmol m^{-2} s^{-1}	
W_j	Electron transport-limited rate of carboxylation	µmol m^{-2} s^{-1}	
W_p	Triose phosphate utilisation-limited rate of carboxylation	µmol m^{-2} s^{-1}	
WUE	Instantaneous water-use efficiency (=A/E)	µmol CO_2 mmol^{-1} H_2O	
iWUE	Intrinsic water-use efficiency (=A/g_{sc})	µmol CO_2 mol^{-1} air	
α	Product of leaf absorptance, the fraction of light directed to PSII and the maximum quantum efficiency of PSII; initial slope of an J/I_{inc} curve	Dimensionless	0.35
θ	Empirical curvature factor	Dimensionless	0.7
λ	Amount of CO_2 released from photorespiration per oxygenation reaction	Dimensionless	0.5
Φ_2	Effective quantum efficiency of PSII electron transport	Dimensionless	0–0.8
Φ_{CO_2}	Maximum quantum efficiency of CO_2 assimilation; initial slope of an A/I_{inc} curve	Dimensionless	0.06
φ	V_o/V_c	mol O_2 mol^{-1} CO_2	0.4
Γ	CO_2 compensation point	µmol CO_2 mol^{-1} air	50
Γ*	CO_2 compensation point in the absence of R_d	µmol CO_2 mol^{-1} air	40

Note: Given are parameter notations and units that are commonly used. The notations largely follow the recommendations of Ely et al. (2021), but other notations may be found in the literature. For example, CO_2 concentrations may be reported in mole fractions (µmol mol^{-1}) or partial pressures (Pa) that have pros and cons in terms of theoretical accuracy and ease of use.

[a]These values are indicative only to give a sense of order of magnitude – they will depend on plant species, age, pretreatment, fertilisation regime, and so forth.

[b]Parameters are reported in two different units, corresponding to CO_2 and O_2 concentrations reported in mole fractions in air (the units required for use in the FvCB model in Box 3) or as concentrations of gases dissolved in liquid, respectively. To convert from one unit to another, the solubility of gases has to be taken into account using Henry's law solubility constants for CO_2 and O_2 (s_c = 0.033 M bar^{-1} and s_o = 0.0013 M bar^{-1} at 25°C [Sander, 2015]; values in the table have been converted to units in M kPa^{-1}).

downstream of the CBB cycle describing the overall sink capacity of the plant. These three parameters are central to modelling A in response to environmental conditions.

A set of parameters describes the maximum rate of net CO_2 or H_2O exchange under specific environmental conditions. For example, A_{max} describes the maximum rate of CO_2 assimilation when light and $[CO_2]$ are saturating and therefore Rubisco oxygenation is largely suppressed. A_{sat} is the net CO_2 assimilation rate at ambient CO_2 concentrations and under light-saturating conditions, and as such is a good indicator of the maximum achievable A under the fluctuating light conditions of the natural environment. The maximum rate of net CO_2 assimilation across a temperature range is denoted A_{opt}. This parameter is useful for functionally characterising the temperature response of net photosynthesis (Yamori et al., 2014).

Concomitant with the assimilatory flux of CO_2 into the leaf, CO_2 is also released from respiration and photorespiration through decarboxylation processes located in the mitochondria, chloroplasts and cytosol (Tcherkez et al., 2017a). The sum of the nonphotorespiratory CO_2 release is, for simplicity and in line with the traditional nomenclature, here referred to as 'mitochondrial' respiration. The rate of respiration in the dark (R_{dark}) varies somewhat throughout the day and night (Gessler et al., 2017), but is overall a good indicator of mitochondrial activity of the leaf. R_{dark} is an important parameter to gauge the overall carbon uptake of a plant over the 24 h diurnal course, since respiration continues throughout the night, countering the carbon gain achieved during the day. Since A is a combination of CO_2 uptake from photosynthesis and CO_2 release from respiration, modelling daytime A in response to environmental conditions requires the knowledge of respiration in the light (R_{light}). Several lines of evidence suggest that respiration is partially inhibited in the light (Tcherkez et al., 2017a, 2017b), highlighting the requirement of a separate measurement of R_{light} to parameterise photosynthesis models. It has also been argued that the discrepancy between R_{dark} and R_{light} may be largely explained by unaccounted-for changes in the chloroplastic CO_2 concentration (C_c) when the light intensity changes (Farquhar & Busch, 2017; Sun et al., 2023), meaning that a measurement of R_{dark} may be sufficient for model parameterisation: R_{dark} and R_{light} generally refer to respiratory fluxes exiting the leaf, while photosynthetic models often are based on the respiratory flux at the intracellular level (denoted R_d). They differ by the amount of CO_2 being refixed before exiting the leaf, which has been estimated at around 24%–38% along the way from the mitochondria to the intercellular space (Busch et al., 2013). Refixation is assumed negligible in the dark and thus R_d can be set to R_{dark} if one assumes that light does not inhibit respiration (but see Buckley et al., 2017). It is noteworthy that as a leaf-level property respiration has the same sign as A, which is a 'positive' flux, despite going in the opposite direction.

2.2 | Instantaneous, or effective, rate and conductance

The most important variables describing the *effective* properties of photosynthesis at a given environmental condition are the instantaneous rates of net CO_2 assimilation (A; often also called A_{net}) and transpiration (E), which can be directly measured with gas exchange (see Box 1). From these variables, one can estimate the instantaneous water-use efficiency (WUE) of a plant under current conditions as the ratio of A to E. The WUE tells us how much carbon the plant gains per unit of water released. However, E is not only dependent on the physiological state of the plant and how open its stomata are, but it is also very strongly influenced by the vapour pressure difference between the inside of the leaf and the surrounding air (VPD$_{leaf}$). As such, E by itself cannot inform us about an intrinsic state of the plant or how WUE might vary with changes in environmental conditions. Therefore, a more physiological description of the trade-off between H_2O loss and CO_2 uptake is the intrinsic water use efficiency (iWUE), which is expressed as the ratio of A to the stomatal conductance (inverse of resistance) to water vapour (g_{sw}).

In addition to the maximum capacities of biochemical parameters, we can obtain from gas exchange the corresponding values that are realised under a given environmental condition. The actual photosynthetic electron transport rate (J_a) relates to the current state of the light-dependent photosynthetic reactions and reflects both the light energy available to drive electron transport and the current capacity to utilise NADPH and ATP produced in the CBB cycle. The activity of the light-independent photosynthetic reactions is represented by the current carboxylation rate (V_c) and oxygenation rate (V_o) of Rubisco. Based on these two parameters one can deduce the fluxes through the CBB cycle and the photorespiratory pathway. Finally, we can quantify the effective rate of triose phosphate utilisation (T_p) under any given environmental condition. All four parameters are not directly measured by gas exchange but are derived from A and E with the help of a biochemical model of photosynthesis as described below.

2.3 | Other properties describing photosynthetic performance

Gas exchange measurements can also deliver additional parameters that have *descriptive properties* and can be useful for comparisons between plants or treatments. These include the incident light intensity (I_{inc}; often also referred to as Q) at which A becomes light-saturated (I_{sat}), the light compensation point (I_c) and CO_2 compensation point (Γ), which describe the light intensity or CO_2 concentration at which photosynthesis and respiration are in balance ($A = 0$), and the leaf temperature (T_{leaf}) at which photosynthesis reaches its optimum (T_{opt}). One can even derive parameters answering 'what if' questions employing limitation analyses that aim to quantify the amount of CO_2 uptake that is forgone due to stomatal or biochemical limitations. For example, the relative stomatal limitation (l_s) explores how much smaller A is due to stomata interfering with CO_2 diffusion, or the relative biochemical limitation (l_b) quantifies the relative effect on A of Rubisco not being fully activated (Grassi & Magnani, 2005).

The long list of parameters explained above, albeit not fully comprehensive, exemplifies the diverse nature of information that can be extracted from photosynthetic gas exchange measurements.

BOX 1   The basis of gas exchange measurements

Most current gas exchange systems are 'open' systems, meaning a continuous stream of gas is blown over a leaf inserted into a well-mixed measurement chamber. Gas properties, chiefly CO_2 and H_2O concentration, are measured by infrared gas analysers (IRGAs) before entering the leaf chamber (reference IRGA) and after exiting the chamber (sample IRGA). Knowing the gas flow rate entering the system (μ_0; $\mu mol\,air\,s^{-1}$) and the area of the leaf enclosed in the chamber (s; m^2), the leaf-level CO_2 assimilation rate (A; $\mu mol\,CO_2\,m^{-2}\,s^{-1}$) and transpiration rate (E; $mmol\,H_2O\,m^{-2}\,s^{-1}$) can then be calculated from the differences in CO_2 and H_2O concentrations between the sample and reference IRGAs (von Caemmerer & Farquhar, 1981; LI-COR, 2022) (Figure Box 1).
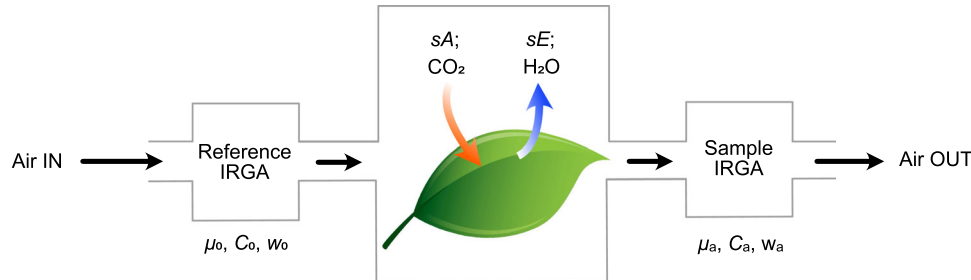

FIGURE BOX 1   General principle of an open gas exchange system. The CO_2 and water vapour concentration (C_0 and w_0, respectively) of the incoming air is measured in a reference IRGA, along with the flow rate of the air entering the leaf chamber (μ_0). These parameters are measured again by the sample IRGA in the air exiting the leaf chamber (C_a, w_a and μ_a). Figure adapted from LI-COR (2022). [Color figure can be viewed at wileyonlinelibrary.com]

The uptake of CO_2 by the leaf is balanced by an efflux of O_2. This is not the case for transpiration, which adds a large amount of water to the chamber. Therefore, the flow rate of gas through the sample IRGA (μ_a) is higher than μ_0 by the amount of water transpired. This allows us to calculate μ_a as:

$$\mu_a = \mu_0 + sE. \tag{1}$$

The total rate of transpiration is calculated from the H_2O concentration ($mmol\,H_2O\,mol^{-1}$ air) inside the reference (w_0) and the sample (w_a) IRGA:

$$sE = \mu_a w_a - \mu_0 w_0. \tag{2}$$

Combining both equations, we can quantify the transpiration rate per leaf area (E) as

$$E = \frac{\mu_0(w_a - w_0)}{s(1 - w_a)}. \tag{3}$$

Similarly, the total rate of net CO_2 uptake inside the chamber is given by

$$sA = \mu_0 C_0 - \mu_a C_a, \tag{4}$$

where C_0 and C_a ($\mu mol\,CO_2\,mol^{-1}$ air) are the CO_2 concentrations inside the reference and sample IRGA, respectively. Frequently, CO_2 (and O_2) concentrations are reported in partial pressures instead of mole fractions. Technically, this is more accurate since the partial pressure of a gas is what determines its availability as substrate for Rubisco (see, e.g., discussion in Sharkey et al., 2007). However, most commonly mole fractions are used for convenience, which is also what we refer to in the following. Substituting μ_a in Equation (4) with Equation (1) and subsequently E with Equation (3) allows us to determine the rate of net CO_2 uptake per leaf area (A) as

$$A = \frac{\mu_0\left(C_0 - C_a\left(\frac{1 - w_0}{1 - w_a}\right)\right)}{s}. \tag{5}$$

It becomes apparent from Equation (5) that accurate measurements of H_2O concentrations are required to obtain accurate CO_2 uptake rates, even if E itself may not be a parameter of interest.

They provide essential information on the physiological status of the plant and can be tracked as the plant ages and develops or responds to environmental factors. To quantify each of these parameters, a certain measurement strategy needs to be followed. While instantaneous photosynthetic, respiratory and transpiratory fluxes can be studied with relatively simple survey measurements, the parameters and traits that define the capacity and limitations for photosynthetic gas exchange require more intricate measurements of the responses of A to environmental parameters, such as $[CO_2]$, light or temperature. In the following we describe which measurements are best suited to obtain the parameters of choice and how to control the IRGA to obtain reliable values.

3 | PHYSIOLOGICAL PRINCIPLES OF PHOTOSYNTHESIS RELEVANT FOR GAS EXCHANGE MEASUREMENTS

Measuring and interpreting photosynthetic gas exchange can be challenging for two main reasons. First, photosynthesis is strongly responsive to light, temperature, humidity and gaseous composition of the air during measurement, which means that these factors need to be tightly controlled and measured in parallel with the measurement of photosynthesis itself. Second, while gas exchange measurements typically determine *net* gaseous exchange, the observations usually reflect several combined *gross* fluxes. For example, net CO_2 exchange combines the CO_2 uptake flux associated with RuBP carboxylation in the CBB cycle, with CO_2 released during respiration and photorespiration. Measurements across a range of different conditions enable us to deconvolute these net fluxes into their gross constituents, which will be further explained in subsequent sections.

The determinants of photosynthetic gas exchange can be divided into diffusional and biochemical limitations. For CO_2 to be fixed by a C_3 plant, it must first traverse a boundary layer of still air surrounding the leaves and subsequently pass through the epidermal layer via stomata to reach the leaf intercellular air space (IAS). From there, a final series of diffusional hurdles await in the form of cell walls, plasma membranes, cytosol, chloroplast envelope and part of the stroma, before the site of CO_2 fixation is reached (see Figure 2). Net CO_2 transfer across this diffusional pathway is driven by gradients in CO_2 concentration from the
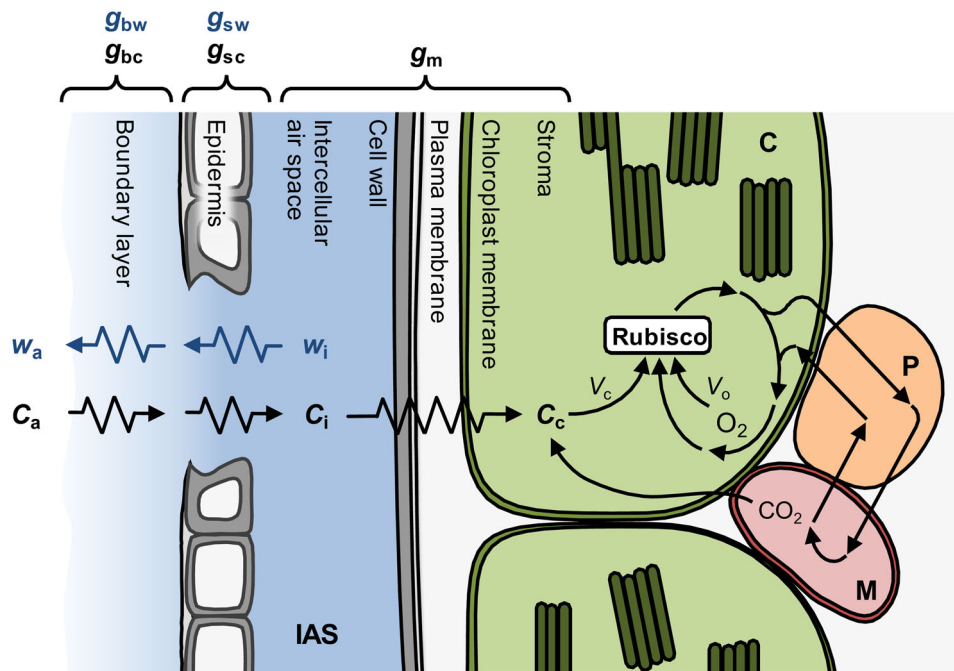
FIGURE 2 Schematic outlining the diffusion of H_2O and CO_2 inside the leaf. Water vapour in the saturated intercellular air space (IAS) (w_i) that exits the leaf through the stomatal pore can be used to quantify the stomatal conductance to H_2O diffusion (g_{sw}) from measurements of the water vapour concentration in the atmosphere (w_a), if the boundary layer conductance to H_2O diffusion (g_{bw}) is known. During gas exchange measurements the boundary layer is minimised in the gas exchange chamber with high-speed fans so it can be reasonably well accounted for by using empirical values. From this, we can describe the path of CO_2 diffusion going the opposite direction into the IAS, with additional information needed to describe the onwards diffusion into the chloroplast (C). The finite conductances to CO_2 diffusion through the boundary layer (g_{bc}), the stomata (g_{sc}) and the mesophyll (g_m) can be viewed as diffusion resistances that cause a progressive decline in CO_2 concentration of the atmosphere (C_a) to that in the IAS (C_i) and the chloroplast (C_c). Both C_c and the chloroplastic oxygen concentration determine the relative rates of Rubisco carboxylation (V_c) and oxygenation (V_o). Following the oxygenation reaction, photorespiratory CO_2 is released from the mitochondria (M) involving some reactions in the peroxisome (P). Figure adapted from Busch (2020) and von Caemmerer (2013). [Color figure can be viewed at wileyonlinelibrary.com]

surrounding air (C_a) to the IAS (C_i) and from there to the chloroplast stroma (C_c). These gradients are established by uptake of CO_2 in the chloroplast stroma via the activity of the CBB cycle and its central enzyme Rubisco, which in turn depends on the provision of ATP and reductant from the photochemical reactions on the chloroplast thylakoid membrane.

To analyse the biochemical limitations to photosynthesis, one first needs to parameterise the diffusional trajectory for CO_2 transfer. In this regard, the parallel measurement of water vapour exchange is needed. Similar to net CO_2 transfer moving into the leaf,

transpiratory water movement out of leaves is determined by diffusion. From the IAS, where water vapour can be assumed saturated (or close to saturated under low to moderate VPD, see Cernusak et al., 2018; Wong et al., 2022), water vapour diffuses out along a gradient of vapour pressure towards the drier air surrounding the leaf. Under most conditions water loss via transpiration is largely associated with diffusional transfer through the stomatal pores, although the observed rate of water release may also include a contribution from water exiting the leaf through the cuticle (Hanson et al., 2016; Márquez et al., 2021, 2022) (see Box 2).

BOX 2   Determinants of photosynthetic gas exchange

At a microscopic level, the local diffusional constraints to cross the pore-studded leaf surface are decided by the proximity to individual stomatal pores. However, at the level of gas exchange measurements, diffusional constraints by all stomata across the measured surface are jointly estimated as stomatal conductance (the inverse of resistance) per unit leaf area and time (g_{sw}). The boundary layer adds another diffusional constraint (boundary layer conductance to water vapour; g_{bw}). Combined, the two yield a total conductance to water vapour (g_{tw}) of:

$$g_{tw} = \frac{1}{\frac{1}{g_{sw}} + \frac{1}{g_{bw}}}. \tag{6}$$

Accounting for ternary effects, we can calculate g_{tw} as (see von Caemmerer & Farquhar [1981] for a detailed derivation):

$$g_{tw} = \frac{E\left(1 - \frac{(w_i - w_a)}{2}\right)}{(w_i - w_a)}, \tag{7}$$

where w_i and w_a are the relative vapour concentrations within the leaf and in the atmosphere, respectively. Here the assumption is that water vapour is at saturation within the leaf and can thus be calculated by knowing the exact leaf temperature. Since the diffusional pathway between the IAS and outside air overlaps between CO_2 and water vapour, measurements of the water flux exiting the leaf can be used to parameterise diffusional resistances to CO_2 entering the leaf. Stomatal conductance to CO_2 diffusion (g_{sc}) can be resolved based on the difference in molar diffusivities between CO_2 and H_2O (CO_2 is a larger molecule and diffuses slower than H_2O) and is described by $g_{sc} = g_{sw}/1.6$. The boundary layer conductance to CO_2 diffusion (g_{sc}) relates to g_{bw} through $g_{bc} = g_{bw}/1.37$ (von Caemmerer & Farquhar, 1981). The total conductance to CO_2 diffusion (g_{tc}) is then described analogous to Equation (6) and can be used to calculate the intercellular CO_2 concentration (C_i) according to

$$C_i = \frac{\left(g_{tc} - \frac{E}{2}\right)C_a - A}{\left(g_{tc} + \frac{E}{2}\right)}. \tag{8}$$

Ignoring boundary layer and ternary effects, Equation (7) can be simplified to provide a transpirational flux from a linear multiplication of the stomatal conductance and the diffusional gradient following Fick's law:

$$E = g_{sw}(w_i - w_a) = g_{sw}\frac{VPD_{leaf}}{P}, \tag{9}$$

where P is atmospheric pressure. Thus, from the observed transpiration flux E and the leaf to air vapour pressure difference (VPD_{leaf}), stomatal conductance to water vapour (g_{sw}) can be resolved. Similarly, Equation (8) can be simplified to describe A according to Fick's law as:

$$A = g_{sc}(C_a - C_i), \tag{10}$$

from which C_i can be estimated. The remainder of the diffusional constraints to CO_2 transfer towards the chloroplast stroma are more difficult to estimate. While these contain an array of different factors (recently reviewed by Evans, 2021), the conductance to get from C_i to C_c is typically summarised in a single parameter called mesophyll conductance to CO_2 (g_m). Although some authors have argued that high resolution CO_2 response curves contain sufficient information to put a number to g_m (Ethier & Livingston, 2004), most researchers rely on additional methods for its estimation, in particular chlorophyll fluorescence and stable isotope discrimination. Using chlorophyll fluorescence to quantify J_a in conjunction with gas exchange allows estimation of C_c based on the apparent partitioning of J_a to photorespiration (Harley et al., 1992), which together with C_i can be used to derive g_m. Alternatively, when discrimination against the stable isotopologue $^{13}CO_2$ relative to $^{12}CO_2$ during photosynthetic CO_2 uptake ($\Delta^{13}C$) is determined in parallel, this can also be used to estimate g_m (Busch et al., 2020; Evans et al., 1986). Analogous to Equation (10), Fick's law then allows calculation of C_c from

$$A = g_m(C_i - C_c). \tag{11}$$

Once C_c is known, the biochemical limitations to photosynthesis can be analysed without the confounding effects of diffusional constraints, allowing for example the determination of in vivo Rubisco activity. Because of the inherent difficulties in quantifying g_m, it is common to use generic values of g_m taken from the literature. Often g_m is also taken as infinite (equivalent to setting $C_c = C_i$), which results in 'apparent' values of the biochemical parameters. Neither approach is ideal, but measurement constraints can make these assumptions unavoidable. In this case, however, it is important to keep in mind that the estimated apparent parameters should not be treated as 'absolute truth', but rather as estimations for comparison purposes. These apparent values are often used for applications in crop improvement (Kromdijk & Long, 2016) or global change models (Rogers et al., 2014).

Inside the chloroplast, Rubisco can react with both CO_2 and O_2. The ratio of Rubisco's carboxylation rate (V_c) to oxygenation rate (V_o) is determined by its kinetic properties and by the the CO_2 and O_2 concentrations (O) inside the chloroplast (Laing et al., 1974):

$$\frac{V_c}{V_o} = \frac{V_{cmax}}{K_c}\frac{K_o}{V_{omax}}\frac{C_c}{O}, \tag{12}$$

where V_{cmax} and V_{omax} are the maximum rates for Rubisco carboxylation and oxygenation and K_c and K_o are the Michaelis–Menten constants for CO_2 and O_2, respectively. The ratio when C_c and O are equal is called the relative specificity of Rubisco ($S_{c/o}$) and given by:

$$S_{c/o} = \frac{V_{cmax}}{K_c}\frac{K_o}{V_{omax}}, \tag{13}$$

$S_{c/o}$ is therefore a property that is determined by the fundamental enzyme kinetics of Rubisco and underpins much of the modelling of photosynthesis. For a given C_c and O, the rate of oxygenation reactions per carboxylation is thus determined by:

$$\phi = \frac{V_o}{V_c} = \frac{1}{S_{c/o}}\frac{O}{C_c}. \tag{14}$$

The parameter ϕ describes how much carbon enters the photorespiratory pathway relative to the CBB cycle and is thus key in modelling gross fluxes of CO_2 from the measured net flux.

4 | MECHANISTIC PHOTOSYNTHESIS MODEL

With the exception of A, R_d and E, most photosynthetic gas exchange parameters cannot be directly measured, but instead are derived from the responses of A to changes in environmental parameters, such as CO_2 concentration or light intensity, with the help of a biochemical model. For C_3 photosynthesis this is done commonly with the model of Farquhar et al. (1980) (henceforth FvCB), described in much detail by von Caemmerer (2000). We provide a concise summary of the FvCB model that adopts some modifications useful for parameter estimation (see Box 3). In its basic form, the FvCB model focusses on the main principles

behind photosynthetic CO_2 uptake and condenses, for example, the entirety of the CBB cycle reactions to the activity of Rubisco. However, the model can be adjusted to address novel questions and needs for parameter estimation (see, e.g., Johnson & Berry, 2021; Tholen et al., 2012; Yin et al., 2021). Many of the photosynthetic parameters discussed here can be quantified by fitting the mechanistic model to experimental data obtained under varying environmental conditions, such as CO_2 concentrations or light intensities.

In turn, A can be predicted under a wide range of environmental conditions with the FvCB model when its photosynthetic parameters are known. Consequently, the FvCB model has been widely integrated into canopy, ecosystem, and global models of carbon flux

BOX 3   Mechanistic photosynthesis model

The FvCB model (Farquhar et al., 1980) describes net CO_2 uptake (A) as the difference between CO_2 uptake from carboxylation (V_c) and CO_2 release following oxygenation (V_o) and respiration (R_d):

$$A = V_c - \lambda V_o - R_d, \tag{15}$$

where λ is the amount of CO_2 released from photorespiration per oxygenation reaction. Most often, it is assumed that $\lambda = 0.5$, or in other words, one molecule of CO_2 is released for every two oxygenation reactions. This is the case when the photorespiratory pathway is closed, that is, no carbon is diverted from it towards other metabolic pathways (but see Busch et al. [2018] and Busch [2020] for when this may not be a good assumption and its impact on λ). The chloroplastic CO_2 compensation point in the absence of respiration (Γ^*), which is the CO_2 concentration where CO_2 uptake from carboxylation equals CO_2 release from photorespiration, can be expressed as (Busch, 2020; Farquhar et al., 1980)

$$\Gamma^* = \frac{\lambda O}{S_{c/o}}. \tag{16}$$

From Equation (16) we can see that Γ^* is determined to a large extent by innate Rubisco kinetic properties (its specificity, $S_{c/o}$), but varies with the current oxygen concentration inside the chloroplast (O) and the overall need for photorespiratory metabolites in other metabolic pathways (encapsulated in λ).

V_c and V_o are difficult to measure directly, but they can be put in relation to each other by combining Equations (14) and (16), which results in

$$\lambda V_o = \frac{\Gamma^*}{C_c} V_c. \tag{17}$$

By substituting Equation (17) into Equation (15), A can then be described as a function of V_c, where the actual carboxylation rate is replaced with the minimum of the potential carboxylation rates that can be supported under a Rubisco, electron transport or triose phosphate utilisation limitation, denoted W_c, W_j and W_p, respectively:

$$A = \min\{W_c, W_j, W_p\}\left(1 - \frac{\Gamma^*}{C_c}\right) - R_d. \tag{18}$$

When RuBP is abundant and not limiting the rate of Rubisco carboxylation, the limiting factor W_c is described by

$$W_c = \frac{V_{cmax} C_c}{C_c + K_c(1 + O/K_o)}. \tag{19}$$

W_c is largely determined by the maximum rate of carboxylation by Rubisco, V_{cmax}, and has thus been termed Rubisco-limited carboxylation rate.

RuBP regeneration can be limited by the availability of either NADPH or ATP, which are both supplied by the light-dependent photosynthetic reactions. Under conditions where the photosynthetic electron transport rate (J) limits the supply of NADPH for the regeneration of RuBP, W_j is given by

$$W_j = \frac{JC_c}{4C_c + 8\Gamma^*}. \tag{20}$$

And finally, RuBP regeneration can be limited by the availability of ATP, which may be controlled by the regeneration of inorganic phosphate through starch and sucrose synthesis from triose phosphates. In this case, the capacity to utilise the assimilated carbon limits the carboxylation rate, and W_p, termed triose-phosphate-utilisation limitation, can be written as

$$W_p = \frac{3T_{pmax} C_c}{C_c - \Gamma^*}, \tag{21}$$

where T_{pmax} is the maximum rate of triose phosphate export from the chloroplast (Harley & Sharkey, 1991). Here, Equations (20) and (21) represent the simplest case assuming a fully closed photorespiratory pathway ($\lambda = 0.5$); both equations need to be modified should this not be the case (see Busch, 2020 for details).

The individual potential net assimilation rates associated with the three potential carboxylation rates and that are fitted to experimental data when using the FvCB model are denoted A_c, A_j and A_p. They are given by:

$$A_c = \frac{V_{cmax}(C_c - \Gamma^*)}{C_c + K_c(1 + O/K_o)} - R_d, \tag{22}$$

$$A_j = \frac{J(C_c - \Gamma^*)}{4C_c + 8\Gamma^*} - R_d \quad \text{and} \tag{23}$$

$$A_p = 3T_{p\,max} - R_d. \tag{24}$$

The relationship between J and J_{max}

A wide range of models have been proposed to relate the potential photosynthetic electron transport rate J at a given light intensity (often written with the light intensity stated as a subscript, see Buckley & Diaz-Espejo, 2015) to its overall maximum capacity (J_{max}). Early models predicting how photosynthesis varies with light intensity were largely empirical. Of those a nonrectangular hyperbola was popularised by Thornley (1976) and Prioul and Chartier (1977) and to date is probably the most widely used model to analyse light response curves:

$$0 = \theta(A + R_d)^2 - (\Phi_{CO_2}I_{inc} + (A_{sat} + R_d))(A + R_d) + \Phi_{CO_2}I_{inc}(A_{sat} + R_d), \tag{25}$$

when adapted to the notation used in our paper and phrased in terms of net instead of gross photosynthesis ($=A + R_d$) to explicitly include respiration. Here, θ is an empirical curvature factor with a value of around 0.7 but that is variable with the measurement CO_2 concentration (Ögren & Evans, 1993). The maximum quantum efficiency for CO_2 assimilation (Φ_{CO_2}) represents the initial slope of the A/I_{inc} curve. Equation (25) can be solved for A as

$$A = \frac{\Phi_{CO_2}I_{inc} + (A_{sat} + R_d) - \sqrt{(\Phi_{CO_2}I_{inc} + (A_{sat} + R_d))^2 - 4\theta\Phi_{CO_2}I_{inc}(A_{sat} + R_d)}}{2\theta} - R_d, \tag{26}$$

which is easily fitted to an entire A/I_{inc} curve to derive A_{sat} (see Supporting Information S1). Equation (25) has been adapted to yield a relationship between J and J_{max} (von Caemmerer, 2000; Farquhar & Wong, 1984):

$$0 = \theta J^2 - (\alpha I_{inc} + J_{max})J + \alpha I_{inc}J_{max}, \tag{27}$$

or when solved for J:

$$J = \frac{\alpha I_{inc} + J_{max} - \sqrt{(\alpha I_{inc} + J_{max})^2 - 4\theta\alpha I_{inc}J_{max}}}{2\theta}. \tag{28}$$

As the maximum quantum yield of electron transport, α is the product of leaf absorptance, the fraction of light directed to PSII and the maximum quantum efficiency of PSII; it corresponds to the initial slope of J versus I_{inc}.

While the above equations are commonly used, we want to promote an idea that integrates more naturally with the FvCB model. This idea is based on one of the earliest approaches to model electron transport that describes J as a function of absorbed light intensity by a rectangular hyperbola (Baly, 1935; Farquhar & von Caemmerer, 1981; Rabinowitch, 1951):

$$J = \frac{\alpha I_{inc}J_{max}}{\alpha I_{inc} + J_{max}}. \tag{29}$$

Note that Equation (29) is a special case of Equation (28) with $\theta = 0$. The rectangular hyperbola was initially discounted for the use with the FvCB model for seemingly underestimating J at intermediate light intensities (Farquhar & von Caemmerer, 1982) and subsequently replaced by other empirical models for J such as nonrectangular hyperbolic functions (see, e.g., Farquhar & Wong, 1984; Smith, 1937) or the photosynthetic rate derived from that (for an overview see, e.g., de Lobo et al., 2013). Recently, however, Johnson and Berry (2021) provided support for the validity of the use of a rectangular hyperbola as a mechanistic description of J and outlined a more detailed model that accounts for cyclic electron transport (CET). Equation (29) can be viewed as a special case of their general model (i.e., when CET is a constant proportion of linear electron transport), which is why we suggest its use if no further detail is available on CET.

Substituting Equation (29) into Equation (20), we obtain an expression of W_j that now refers to the inherent biochemical properties of electron transport rather than the J realised under a given environment. This leads to an equation for the RuBP regeneration-limited CO_2 assimilation rate A_j that can be used to fit J_{max} from A/I_{inc} curves:

$$A_j = \left(\frac{\alpha I_{inc} J_{max}}{\alpha I_{inc} + J_{max}} \right) \left(\frac{C_c - \Gamma^*}{4C_c + 8\Gamma^*} \right) - R_d. \tag{30}$$

Importantly, in contrast to the nonrectangular model (Equation 26) that derives J_{max} from the entire A/I_{inc} curve (see, e.g., de Lobo et al., 2013; Ögren & Evans, 1993), Equation (30) is applied only to the light-limited portion of an A/I_{inc} curve, with the remainder of the curve fitted by Equations (22) or (24) (see Supporting Information S1). The two types of models yield substantially different outcomes when J_{max} is estimated from fitting experimental data (see Fig. S2), making the choice of model an important decision. Because this rectangular model (Equations 29 and 30) is both mechanistic (assuming CET is proportional to J) and directly compatible with the FvCB model, we suggest its use instead of the empirical nonrectangular model for fitting A/I_{inc} curves or when relating J to J_{max}. Nevertheless, in some cases it may be useful to employ alternative models, for example, to maintain consistency with previous measurements or when parameters other than J_{max} are required.

(Bernacchi et al., 2013; Rogers et al., 2014; Walker et al., 2014). The centrality of photosynthetic gas exchange parameters to earth system models has resulted in immense efforts to characterise genetic, developmental and environmental variation in the model parameters (Medlyn et al., 1999; Poorter et al., 2022; Rogers, 2014).

5 | TYPES OF MEASUREMENTS SUITABLE FOR ESTIMATING INDIVIDUAL PHOTOSYNTHETIC PARAMETERS

In the previous sections, we discussed the main photosynthetic parameters that can be derived from gas exchange measurements and how they relate to our understanding of photosynthetic function. A series of 'how-to' experimental procedures to reliably estimate each of these photosynthetic parameters is outlined in Supporting Information S1. This includes procedures for survey measurements, A/C_i responses, A/I_{inc} responses, A/T responses, Laisk and Kok measurements, as well as a brief description of other photosynthesis measurements that are less commonly applied. For the recommendations in Supporting Information S1, we have summarised what we, on balance, consider 'best practice'. However, it is important to reiterate that different questions will require different measurement approaches and each experimental setup will have different limitations on equipment and time available that will necessitate compromises. Our recommendations are therefore to be viewed as a starting point for designing a customised approach.

6 | MODEL FITTING ROUTINES TO ESTIMATE PHOTOSYNTHETIC PARAMETERS

Estimates of the photosynthetic capacity parameters from CO_2 response curves (i.e., V_{cmax}, J and T_{pmax}) and light response curves (J_{max}) are obtained via a nonlinear curve fitting routine to minimise

the difference between the collected CO_2 assimilation data (A) to the underlying predicted A modelled from FvCB equations (Equation 18). Commonly used tools for data analysis include Excel spreadsheet-based methods to fit photosynthetic response curves (Bellasio et al., 2016a, 2016b; de Lobo et al., 2013; Sharkey, 2016; Sharkey et al., 2007), R packages (e.g., *plantecophys*, *plantecowrap*, *photosynthesis* and *msuRACiFit*) to obtain similar nonlinear fitting outputs (Duursma, 2015; Gregory et al., 2021; Stinziano et al., 2021), and even online services that return fitted data (e.g., leafweb.org; Gu et al., 2010). Although standard A/C_i curve fitting procedures are based on the same theory regardless of the tool used, differences in parameter estimates arise due to method specific inherent assumptions and drawbacks. For example, spreadsheet-based fitting tools (Sharkey et al., 2007) are accessible to many physiologists comfortable with the Excel solver add-on, but require users to make judgements about limiting factors and specify the transition from RuBP-saturated to RuBP-limited A to solve for V_{cmax} and J separately. Due to this, estimates using this method require subjective decision making that relies on user experience, and each curve must be analysed independently. While this approach enables a deep understanding of the data that support each measurement, it hinders large-scale analysis. The widely used *plantecophys* R package circumvents the need for a priori assignment of data limitations by fitting the data to the hyperbolic minimum of A_c, A_j, and A_p over the entire CO_2 range collected, though the transition point can be fixed to check the fit against assumptions. A major advantage of moving to coding based, rather than spreadsheet based, curve fitting procedures is a decrease in analysis time per curve and increase in throughput, reproducibility and shareability, though this depends on user comfort with the programming language. Next generation R packages are now emerging, including *photosynthesis*, which contain not only functionality to fit A/C_i curves, but also A/I_{inc} curves, R_{light}, mesophyll and stomatal conductance, and hydraulic curves (Stinziano et al., 2021). A note of caution is warranted at this point: Parameter notation may not be standardised between the different statistical packages and

may differ from this paper. Similarly, differences exist in the functions used to fit the data, in particular those used to fit A/I_{inc} responses.

The accuracy of the FvCB model depends on proper representation of the kinetic properties of Rubisco and requires an estimate of Rubisco Michaelis–Menten constants (K_c, K_o or the effective value in air K_m) and Γ^*, as well as their temperature dependence (Equations 22 and 23). Many species-specific estimates of these parameters have now been obtained from in vitro measurements, showing substantial variation among species (Galmés et al., 2016; Hermida-Carrera et al., 2016; Orr et al., 2016; Sharwood et al., 2016). However, using in vitro estimates of Rubisco kinetic temperature responses can produce modelled values for A that deviate from observed measurements as temperatures move to warm and cool extremes (Bernacchi et al., 2001). Using these temperature functions requires assumptions about in vivo conditions, such as pH and CO_2 diffusion to the site of carboxylation and can be further complicated by differences in in-vitro assay conditions (Boyd et al., 2019; Iñiguez et al., 2021). On the other hand, however, in vitro-derived kinetic parameters do not come with the requirement of having to know C_c or the amount of CO_2 released per Rubisco oxygenation reaction (λ), which may be the most important source of error. Whether the chosen set of parameters yields not just a close fit but also an appropriate fit can be checked by the sensitivity of photosynthesis to changes in the O_2 or CO_2 concentration, which can independently determine the underlying photosynthetic limitation (Busch & Sage, 2017).

A further parameter impacting estimates from CO_2 response curves is mesophyll conductance (g_m), which impacts the effective partial pressure of CO_2 inside the chloroplast and will therefore affect the fitted V_{cmax}. A low g_m decreases the curvature of the A/C_i curve and can be accounted for in both spreadsheet and coding-based curve-fitting tools if an independent measurement is available (Duursma, 2015; Sharkey et al., 2007). If an independent measurement is not available, g_m can be estimated by substituting C_c with (C_i – A/g_m) in Equations 22 and 23 and using nonlinear curve fitting to minimise the difference from the observed data. Independent g_m measurements can be obtained, for example, with stable carbon isotope techniques, by combining gas exchange with chlorophyll fluorescence measurements, or with curve-fitting methods (Busch et al., 2020; Pons et al., 2009; Yin & Struik, 2009). While the curve-fitting methods assume g_m to be constant, the stable carbon isotope technique can be used to assess how g_m varies across environmental conditions (Busch et al., 2020).

7 | GOOD PRACTICE FOR THE GAS EXCHANGER

7.1 | Perform premeasurement checks

During warmup of the machine, perform the tests recommended by the manufacturer. This may include checking for accuracy and responsiveness of temperature parameters and sensors, light control and functioning of the chamber mixing fan.

7.2 | Have the machine well calibrated

The signal from an IRGA can drift through time due to ageing (e.g., reduced infrared light intensity) or due to attenuation by the accumulation of particles (e.g., dust) absorbing infrared. In addition to regularly zeroing the IRGAs for both CO_2 and H_2O, it is a good practice to calibrate the IRGA against reference gases with low and high concentrations (intercept and slope) before a measurement campaign or when maintenance has been performed on the IRGA (e.g., cleaning of the optical bench). Using the same calibration gas for different machines enables an increase in the measurement accuracy and a reduction in the interinstrument bias.

7.3 | Check for leaks

It is imperative to check for leaks after each time the chamber is clamped onto a leaf. Porous gasket material can absorb/release CO_2 and H_2O, which leads to small fluxes in and out of the chamber (Long & Hällgren, 1993). The relative impact of these diffusive fluxes is exacerbated at the high and low [CO_2] conditions used in CO_2 response curves. This can often be corrected for if the external CO_2 is known (see the manufacturer's documentation). A second type of leak is created by the gasket not perfectly fitting the shape of the leaf (especially the major veins), causing small pores at the gasket-leaf interface (Long & Bernacchi, 2003). To detect such leaks, exhaled air should be blown near the chamber while monitoring the [CO_2] within the chamber. The absence of spikes in the trace for the [CO_2] within the chamber is a good indicator that major leaks are absent. If the leaf cannot be repositioned in the chamber to avoid leaks, vacuum grease can be used with care to seal the chamber. If a leak cannot be avoided, several methods have been proposed to partially correct for it (Boesgaard et al., 2013; Flexas et al., 2007; Gong et al., 2015; Kitao et al., 2017; Long & Bernacchi, 2003).

7.4 | Check gasket condition

Gasket materials are generally elastic to fit the shape of the leaf. However, they can move from their original position or flatten with time, which reduces their efficiency to maintain a good seal with the leaf. It is recommended to leave the chamber slightly open when no measurement is performed or during storage to prolong the gasket life.

7.5 | Check for stability during the measurement

When performing leaf gas exchange, it is important that the [CO_2] and [H_2O] of the incoming air into the chamber are stable at least over short periods of time (minutes). If the machine does not automatically control this with a mixer, rapid fluctuations can be dampened and stable concentrations can be achieved by using a

buffer volume, for example, a large sealed plastic bucket placed in the air stream before the machine air intake.

7.6 | Monitor system parameters

Chamber conditions can change quickly and unintentionally, for example, leaf temperature can rapidly increase with light intensity, which influences VPD_{leaf} as well. Dynamically controlling leaf temperature rather than keeping the chamber temperature constant will avoid variation in T_{leaf} but can induce transient artefacts in the measurement (e.g., large spike in stomatal conductance) after a change in light intensity, as rapid changes in incoming air temperature and water vapour reach a new equilibrium with the conditions in the chamber. Changes in g_s and/or VPD_{leaf} will also affect the relative humidity (RH) of the chamber air and potentially reach saturation. Thus the dew point temperature within the chamber is important to monitor to avoid condensation, especially at low flow rate and high leaf transpiration. Monitoring the data as it comes in is also important so that, for example, closing stomata or a CO_2 cartridge that is running out can be noticed before too much time has passed and the measurement needs to be repeated.

7.7 | Maximise signal to noise ratio

While a high flow rate within the chamber is preferable for faster measurement response, it also decreases the $[CO_2]$ and $[H_2O]$ differential measured between the reference and sample IRGAs. When the difference in concentration becomes too small, calculated data such as photosynthesis and stomatal conductance become noisy when the detection limit of the IRGA is larger than the difference measured. Reducing the airflow going through the chamber can increase the differential and benefit the signal to noise ratio. However, this simultaneously increases the influence of potential leaks on the measurement due to a longer residence time of the air inside the chamber and a lower chamber pressure that exacerbates diffusive leaks across the gasket. A lower flow rate also results in larger importance of leaf transpiration on humidity control within the chamber, as water vapour accumulates. It is recommended to start with flow rate values recommended by the manufacturer and to adjust them based on the leaf response.

7.8 | Adjust light quality

The actinic light source is often composed of a combination of red and blue wavelengths. For a long time, the default was a high proportion of red light to drive photosynthesis (90%) and a small amount of blue light to stimulate stomatal opening (10%). As leaf absorbance is dependent on the wavelengths, different ratios of red and blue light intensity result in different photosynthesis values (Evans et al., 2017). The classic view on the importance of red and

blue light has been challenged as some species do not respond to blue light (Vialet-Chabrand et al., 2021) and other wavelengths such as green and far-red light may play an important role in driving photosynthesis (Smith et al., 2017; Zhen & Bugbee, 2020).

7.9 | Match IRGAs

Depending on the gas exchange system used, CO_2 and H_2O in and out of the chamber may be measured by two separate IRGAs, which can introduce a systematic bias if their calibration or response slightly differ. To overcome this problem, the same air is passed through both IRGAs simultaneously and the concentration readings are electronically 'matched' to the same values. Matching IRGAs is generally performed after changes in $[CO_2]$ and/or $[H_2O]$ or after a set time (e.g., 30 min). Matching too often, especially when there are transient changes in $[CO_2]$ and/or $[H_2O]$ may not result in more accurate measurements. It is often best to wait for stable measurements before matching (but this is system dependent, check the manufacturer's manual). For long term measurements (e.g., diurnal kinetics), it is important to match regularly as the temporal drift of the IRGA may hamper interpretations.

7.10 | Select appropriate chamber size

Ideally, the size of the gas exchange chamber used should be proportional to the leaf dimensions as the setup is generally easier to handle when the leaf covers the entire area of the chamber. There is a trade-off between smaller chambers that have quicker response times due to their smaller air volume (Weiss et al., 2009) and larger chambers that are less influenced by the leaf heterogeneity (e.g., stomatal patchiness; Mott & Buckley, 2000). Stomatal patchiness is a spatial or temporal heterogeneity that may be caused by hydraulic interactions between adjacent stomatal pores (Peak et al., 2023) and that influences the accuracy of estimated intercellular CO_2 concentrations. The size of the gas exchange chamber should therefore be matched to the requirements and purposes of the experiment.

7.11 | Chamber mixing fan speed

The mixing fan decreases the boundary layer around the leaf. High mixing fan speeds reduce the boundary layer to a minimum and ensuring the chamber air is well mixed, thereby decreasing the uncertainty in true g_s values. When using a custom chamber setup, use a powerful fan to ensure good mixing of the chamber air. It is worth keeping in mind that for a given VPD_{leaf} a decreased boundary layer inside the chamber means that the leaf is losing more water than a leaf placed outside the chamber, which may affect g_s when given enough time. A leaf inside the chamber thus does not experience the 'same environment' as a leaf outside the chamber, even though the environmental conditions may be the same.

In addition to the effects on boundary layer, high fan speeds facilitate the heat exchange between the the air and the leaf surface as well as the chamber wall. Low fan speeds may become an issue when measuring at temperatures below ambient, where inhibited heat exchange can lead to undercooling of the chamber and subsequent condensation issues.

7.12 | Keeping the chamber clean

Dust and dirt in the chamber can absorb and release gases, interfering with the measurements especially when conditions in the chamber are rapidly changing. When foreign bodies accumulate in the IRGA, they cause noise in the signal and attenuate its strength. Small animals (e.g., spiders, thrips) can cause erratic spikes in the signal and thus it is important to check the leaf surface before inserting it into the chamber. Leaves that are damaged by pests or wounded should not be measured as they can display a high transpiration rate that is not the result of a stomatal aperture. When measuring in the field, ensure the console is raised off the ground to minimise dust entering the system via the air intake.

7.13 | Regular chemical check

Before starting a new series of measurements, it is important to use fresh chemicals (i.e., soda-lime and silica gel/drierite) to avoid environmental control issues during the measurements. Most of the chemicals have a colour indicator allowing to detect when replacement is needed. Blowing into the air inlet while establishing conditions for IRGA zeroing can help to assess the condition of the soda-lime: no CO_2 should make it past the scrub bottle when on full scrub.

7.14 | Correct for measured leaf area

In some cases, the leaf within the chamber does not cover the entire measurement area and a value needs to be manually determined and entered. The area can be derived from a picture of the leaf inside the chamber (if it is a clear top chamber) or by marking the position of the gasket with a pen and taking a picture with a similar loose gasket. Imaging software, such as the open source image processing package Fiji (Schindelin et al., 2012), can then be used to estimate the area (Savvides & Fotopoulos, 2018). For grass leaves, knowing the width at each side of the chamber is often enough to estimate the area based on a rectangular shape. As photosynthetic fluxes are area-based, errors in leaf area estimates are to be avoided.

7.15 | Selection of leaves to be measured

In most studies, the most recent fully expanded leaf is used to perform the measurement. However, within the plant canopy there are large variations in photosynthetic capacity due to light gradients and differences in leaf age. It is therefore important to be consistent in the choice of the leaf to measure between plants and to consider temporal factors such as leaf ageing for long experiments.

8 | PITFALLS TO AVOID

8.1 | Condensation

Condensation can occur as the dewpoint temperature of the chamber air approaches the lowest temperature of any system component, which is usually the chamber wall temperature. Even though condensation can often not be visually seen directly, it still causes invalid photosynthesis measurements. Once condensation is detected, the machine needs to dry out before any further measurements take place. To ensure good humidity control, before measurements make sure desiccant is fresh and the IRGAs are properly zeroed. During measurements, we advise that the RH should not exceed 85%. Controlling the humidity by ensuring the dew point temperature of the air is always at least one degree lower than the minimum of leaf, air or chamber temperature will prevent high RH and condensation forming in the measuring chamber – pay special attention to the temperature of the chamber block, as this is the most likely place where condensation may occur. Take particular note in the minutes after closing a leaf into the chamber to ensure transpiration does not cause high RH when stomata acclimate to the new conditions. If the set humidity cannot be maintained with the humidity control alone and needs to be reduced, the temperature and/or flow rate can be increased.

8.2 | Negative C_i values

As a mole fraction of CO_2 molecules in air, C_i values should always be positive. If condensation occurs in the leaf chamber C_i calculations may be incorrect and negative C_i values can occur. The danger of this happening is particularly high during CO_2 response curves at low $[CO_2]$, when stomata tend to be opened the most. On machines that do not automatically adjust RH to prevent condensation follow the tips above for avoiding condensation in the leaf chamber.

8.3 | Leaks

Leaks occur mainly through the gasket securing the leaf in the measuring head, through unsecure exhaust tubing, damaged O-rings at measuring head connection points and poor seals on desiccant columns. Flow rates unable to reach set point and fluctuating CO_2 values unable to reach set points higher than atmospheric CO_2 values may indicate a leak. If a leak is suspected carry out the following checks (also see section on 'good practice'):

1. Is the measuring head correctly closed and gaskets intact? Replace gaskets if compression is causing a poor seal.
2. Is exhaust tubing correctly attached to measuring head and console?
3. Are humidifier and desiccant columns correctly in place and caps sealed with air filters intact?
4. Is the thermocouple correctly installed?
5. Check all O-rings and replace any that are damaged.

8.4 | Closed stomata

If g_s is too low, for example, when the plant is drought-stressed, obtaining high C_i values and thus a useful A/C_i response can be challenging. For these measurements it is important to properly adjust VPD_{leaf}, as excessive transpiration is a major contributor to stomatal closing: Generally, VPD_{leaf} should not exceed 1.5 kPa to avoid stomatal closure, while condensation needs to be avoided by ensuring RH does not exceed 85%. A range of VPD_{leaf} suitable for most measurements is around 0.8–1.2 kPa. An appropriate level of VPD_{leaf} is also dependent on whether the machine has to heat or cool the chamber to reach the set measurement temperature. RH of 85% may be suitable in the former and reach condensation in the latter case. It helps to keep plants well-watered and not expose them to a sudden temperature/humidity change right before the measurement. If despite this, stomata are very slow to respond, check the light quality settings (the contribution of blue light should be at least 10%, see 'Adjust light quality' above). The leaf can also be briefly exposed to low $[CO_2]$ (~100 µmol mol^{-1}), which helps induce stomatal opening.

8.5 | Large temperature gradient between ambient air and inside of chamber

Large gradients between the temperature of the console, where the measuring air is conditioned, and the temperature set inside the chamber bear the danger of condensation (if the chamber block has to cool down hot incoming air) or of not being able to reach a VPD_{leaf} low enough to ensure open stomata (if cold air coming from console cannot carry enough humidity, despite being close to saturated). In addition, large temperature gradients between the chamber air and the leaf may cause T_{leaf} to be incorrect, as the temperature measured by the leaf thermocouple will be influenced by the surrounding air temperature (Mott & Peak, 2011). These problems can be minimised by keeping all system components as close as possible to the set T_{leaf}. For measurements far outside of ambient conditions, the whole gas exchange console and measuring head should be placed within a climate-controlled space, such as a growth chamber or incubator. Then the temperature surrounding the IRGA can be set close to T_{leaf}, minimising temperature gradients and condensation as well as extending the temperature range for measurements.

8.6 | Thermocouple position on the leaf

The leaf thermocouple must be installed correctly and touching the abaxial surface of the leaf during the measurement. If not touching the leaf, it will measure air temperature in the chamber instead. If pushed too far it could tear the leaf and bend the thermocouple. For larger chambers a single thermocouple may not be sufficient to capture heterogeneities across the leaf – use a second thermocouple when given the option. Accurate leaf temperature measurements are required for computation of many parameters including g_s and C_i, and measurements from an incorrectly placed or damaged thermocouple can cause incorrect estimation of photosynthetic capacities from curve fitting. In situations where contact with the leaf surface is not possible, an energy balance method can be used to estimate parameters.

8.7 | Time of day effects

Many species operate on a diurnal cycle, some with a noted midday depression of photosynthesis due to stomatal closure (Panda, 2011; Hirasawa & Hsiao, 1999) or enhanced photoprotection or photo-inhibition (Ögren & Rosenqvist, 1992) in hot and high-light conditions. When comparing photosynthetic capacities between samples ensure measurements are made when g_s is not excessively limiting photosynthesis, that is, when stomata are largely open. Observing diurnal patterns of g_s for the species of interest prior, by taking sets of survey measurements over the course of a day, can help to determine what time of day is most appropriate for making measurements (Matthews et al., 2018).

8.8 | Measuring attached versus detached leaves

It is preferable to measure attached leaves as cutting the leaf can result in an immediate change in leaf water potential that influences transpiration and stomatal conductance responses. For specific treatments (e.g., application of hormones) or due to logistic limitation, measurements on detached leaves can be performed but care should be taken with interpretation of such results, especially those relying on g_s (Ferguson et al., 2023).

ORCID
Florian A. Busch http://orcid.org/0000-0001-6912-0156
Elizabeth A. Ainsworth http://orcid.org/0000-0002-3199-8999
Anna Amtmann http://orcid.org/0000-0001-8533-121X

Amanda P. Cavanagh http://orcid.org/0000-0001-5918-8093

Steven M. Driever http://orcid.org/0000-0003-4144-6028

John N. Ferguson http://orcid.org/0000-0003-3603-9997

Johannes Kromdijk http://orcid.org/0000-0003-4423-4100

Tracy Lawson http://orcid.org/0000-0002-4073-7221

Andrew D. B. Leakey http://orcid.org/0000-0001-6251-024X

Jack S. A. Matthews http://orcid.org/0000-0002-7282-8929

Katherine Meacham-Hensold http://orcid.org/0000-0003-1198-5389

Richard L. Vath http://orcid.org/0000-0002-3641-5967

Silvere Vialet-Chabrand http://orcid.org/0000-0002-2105-2825

Berkley J. Walker http://orcid.org/0000-0001-5932-6468

Maria Papanatsiou http://orcid.org/0000-0003-1871-9497

REFERENCES

Ainsworth, E.A. & Long, S.P. (2005) What have we learned from 15 years of free-air CO_2 enrichment (FACE)? A meta-analytic review of the responses of photosynthesis, canopy properties and plant production to rising CO_2. *New Phytologist*, 165, 351–372.

Ball, J.T., Woodrow, I.E. & Berry, J.A. (1987) A model predicting stomatal conductance and its contribution to the control of photosynthesis under different environmental conditions. In: Briggins, J. (Ed.) *Progress in Photosynthesis Research*. Dordrecht: Martinus Nijhoff Publishers, pp. 221–224.

Baly, E.C.C. (1935) The kinetics of photosynthesis. *Proceedings of the Royal Society of London, Series B: Biological Sciences*, 117, 218–239.

Bellasio, C., Beerling, D.J. & Griffiths, H. (2016a) An Excel tool for deriving key photosynthetic parameters from combined gas exchange and chlorophyll fluorescence: theory and practice. *Plant, Cell & Environment*, 39, 1180–1197.

Bellasio, C., Beerling, D.J. & Griffiths, H. (2016b) Deriving C_4 photosynthetic parameters from combined gas exchange and chlorophyll fluorescence using an Excel tool: theory and practice. *Plant, Cell & Environment*, 39, 1164–1179.

Bernacchi, C.J., Bagley, J.E., Serbin, S.P., Ruiz-Vera, U.M., Rosenthal, D.M. & Vanloocke, A. (2013) Modelling C_3 photosynthesis from the chloroplast to the ecosystem. *Plant, Cell & Environment*, 36, 1641–1657.

Bernacchi, C.J., Singsaas, E.L., Pimentel, C., Portis, A.R. & Long, S.P. (2001) Improved temperature response functions for models of Rubisco-limited photosynthesis. *Plant, Cell & Environment*, 24, 253–259.

Bloom, A.J., Mooney, H.A., Björkman, O. & Berry, J. (1980) Materials and methods for carbon dioxide and water exchange analysis. *Plant, Cell & Environment*, 3, 371–376.

Boesgaard, K.S., Mikkelsen, T.N., Ro-Poulsen, H. & Ibrom, A. (2013) Reduction of molecular gas diffusion through gaskets in leaf gas exchange cuvettes by leaf-mediated pores. *Plant, Cell & Environment*, 36, 1352–1362.

Boyd, R.A., Cavanagh, A.P., Kubien, D.S. & Cousins, A.B. (2019) Temperature response of Rubisco kinetics in *Arabidopsis thaliana*: thermal breakpoints and implications for reaction mechanisms. *Journal of Experimental Botany*, 70, 231–242.

Buckley, T.N. & Diaz-Espejo, A. (2015) Reporting estimates of maximum potential electron transport rate. *New Phytologist*, 205, 14–17.

Buckley, T.N., Vice, H. & Adams, M.A. (2017) The Kok effect in *Vicia faba* cannot be explained solely by changes in chloroplastic CO_2 concentration. *New Phytologist*, 216, 1064–1071.

Busch, F.A. (2020) Photorespiration in the context of Rubisco biochemistry, CO_2 diffusion and metabolism. *The Plant Journal*, 101, 919–939.

Busch, F.A. (2018) Photosynthetic gas exchange in land plants at the leaf level. In: Covshoff, S. (Ed.) *Photosynthesis: methods and protocols*. New York, USA: Springer, pp. 25–44.

Busch, F.A., Holloway-Phillips, M., Stuart-Williams, H. & Farquhar, G.D. (2020) Revisiting carbon isotope discrimination in C_3 plants shows respiration rules when photosynthesis is low. *Nature Plants*, 6, 245–258.

Busch, F.A. & Sage, R.F. (2017) The sensitivity of photosynthesis to O_2 and CO_2 concentration identifies strong Rubisco control above the thermal optimum. *New Phytologist*, 213, 1036–1051.

Busch, F.A., Sage, R.F. & Farquhar, G.D. (2018) Plants increase CO_2 uptake by assimilating nitrogen via the photorespiratory pathway. *Nature Plants*, 4, 46–54.

Busch, F.A., Sage, T.L., Cousins, A.B. & Sage, R.F. (2013) C_3 plants enhance rates of photosynthesis by reassimilating photorespired and respired CO_2. *Plant, Cell & Environment*, 36, 200–212.

von Caemmerer, S. (2000) *Biochemical models of leaf photosynthesis*. Collingwood, Australia: CSIRO Publishing.

von Caemmerer, S. (2013) Steady-state models of photosynthesis. *Plant, Cell & Environment*, 36, 1617–1630.

von Caemmerer, S. & Farquhar, G.D. (1981) Some relationships between the biochemistry of photosynthesis and the gas exchange of leaves. *Planta*, 153, 376–387.

Carter, K.R., Wood, T.E., Reed, S.C., Butts, K.M. & Cavaleri, M.A. (2021) Experimental warming across a tropical forest canopy height gradient reveals minimal photosynthetic and respiratory acclimation. *Plant, Cell & Environment*, 44, 2879–2897.

Cernusak, L.A., Ubierna, N., Jenkins, M.W., Garrity, S.R., Rahn, T., Powers, H.H. et al. (2018) Unsaturation of vapour pressure inside leaves of two conifer species. *Scientific Reports*, 8, 7667.

Coast, O., Posch, B.C., Bramley, H., Gaju, O., Richards, R.A., Lu, M. et al. (2021) Acclimation of leaf photosynthesis and respiration to warming in field-grown wheat. *Plant, Cell & Environment*, 44, 2331–2346.

Dillaway, D.N. & Kruger, E.L. (2010) Thermal acclimation of photosynthesis: a comparison of boreal and temperate tree species along a latitudinal transect. *Plant, Cell & Environment*, 33, 888–899.

Duursma, R.A. (2015) Plantecophys – an R package for analysing and modelling leaf gas exchange data. *PLoS One*, 10, e0143346.

Ely, K.S., Rogers, A., Agarwal, D.A., Ainsworth, E.A., Albert, L.P., Ali, A. et al. (2021) A reporting format for leaf-level gas exchange data and metadata. *Ecological Informatics*, 61, 101232.

Ethier, G.J. & Livingston, N.J. (2004) On the need to incorporate sensitivity to CO_2 transfer conductance into the Farquhar-von Caemmerer-Berry leaf photosynthesis model. *Plant, Cell & Environment*, 27, 137–153.

Evans, J.R. (2021) Mesophyll conductance: walls, membranes and spatial complexity. *New Phytologist*, 229, 1864–1876.

Evans, J.R., Morgan, P.B. & von Caemmerer, S. (2017) Light quality affects chloroplast electron transport rates estimated from chl fluorescence measurements. *Plant and Cell Physiology*, 58, 1652–1660.

Evans, J.R. & Santiago, L.S. (2014) PrometheusWiki gold leaf protocol: gas exchange using LI-COR 6400. *Functional Plant Biology*, 41, 223–226.

Evans, J.R., Sharkey, T.D., Berry, J.A. & Farquhar, G.D. (1986) Carbon isotope discrimination measured concurrently with gas-exchange to investigate CO_2 diffusion in leaves of higher plants. *Australian Journal of Plant Physiology*, 13, 281–292.

Farquhar, G.D. & Busch, F.A. (2017) Changes in the chloroplastic CO_2 concentration explain much of the observed Kok effect: a model. *New Phytologist*, 214, 570–584.

Farquhar, G.D. & von Caemmerer, S. (1981) Electron transport limitations on the CO_2 assimilation rate of leaves: a model and some observations in *Phaseolus vulgaris* L. In: Akoyunoglou, G. (Ed.) *Photosynthesis: Proceedings of the Fifth International Congress on*

Photosynthesis. Philadelphia, USA: Balaban International Science Services, pp. 163–175.

Farquhar, G.D. & von Caemmerer, S. (1982) Modelling of photosynthetic response to environmental conditions. In: Lange, O.L., Nobel, P.S., Osmond, C.B. & Ziegler, H. (Eds.) *Physiological plant ecology II*. Heidelberg: Springer-Verlag, pp. 549–587.

Farquhar, G.D., von Caemmerer, S. & Berry, J.A. (1980) A biochemical model of photosynthetic CO_2 assimilation in leaves of C_3 species. *Planta*, 149, 78–90.

Farquhar, G.D. & Wong, S. (1984) An empirical model of stomatal conductance. *Functional Plant Biology*, 11, 191–210.

Ferguson, J.N., Jithesh, T., Lawson, T. & Kromdijk, J. (2023) Leaf excision introduces limited and species-specific effects on photosynthetic parameters across crop functional types. *Journal of Experimental Botany*, 74, 6662–6676.

Flexas, J., Diaz-Espejo, A., Berry, J., Cifre, J., Galmes, J., Kaldenhoff, R. et al. (2007) Analysis of leakage in IRGA's leaf chambers of open gas exchange systems: quantification and its effects in photosynthesis parameterization. *Journal of Experimental Botany*, 58, 1533–1543.

Gaastra, P. (1959) *Photosynthesis of crop plants as influenced by light, carbon dioxide, temperature, and stomatal diffusion resistance*. H. Veenman & Zonen N.V., Wageningen, The Netherlands.

Galmés, J., Hermida-Carrera, C., Laanisto, L. & Niinemets, Ü. (2016) A compendium of temperature responses of Rubisco kinetic traits: variability among and within photosynthetic groups and impacts on photosynthesis modeling. *Journal of Experimental Botany*, 67, 5067–5091.

Gessler, A., Roy, J., Kayler, Z., Ferrio, J.P., Alday, J.G., Bahn, M. et al. (2017) Night and day – circadian regulation of night-time dark respiration and light-enhanced dark respiration in plant leaves and canopies. *Environmental and Experimental Botany*, 137, 14–25.

Gong, X.Y., Schäufele, R., Feneis, W. & Schnyder, H. (2015) $^{13}CO_2/^{12}CO_2$ exchange fluxes in a clamp-on leaf cuvette: disentangling artefacts and flux components. *Plant, Cell & Environment*, 38, 2417–2432.

Grassi, G. & Magnani, F. (2005) Stomatal, mesophyll conductance and biochemical limitations to photosynthesis as affected by drought and leaf ontogeny in ash and oak trees. *Plant, Cell & Environment*, 28, 834–849.

Gregory, L.M., McClain, A.M., Kramer, D.M., Pardo, J.D., Smith, K.E., Tessmer, O.L. et al. (2021) The triose phosphate utilization limitation of photosynthetic rate: out of global models but important for leaf models. *Plant, Cell & Environment*, 44, 3223–3226.

Gu, L., Pallardy, S.G., Tu, K., Law, B.E. & Wullschleger, S.D. (2010) Reliable estimation of biochemical parameters from C_3 leaf photosynthesis-intercellular carbon dioxide response curves. *Plant, Cell & Environment*, 33, 1852–1874.

Hanson, D.T., Stutz, S.S. & Boyer, J.S. (2016) Why small fluxes matter: the case and approaches for improving measurements of photosynthesis and (photo)respiration. *Journal of Experimental Botany*, 67, 3027–3039.

Harley, P.C., Loreto, F., Dimarco, G. & Sharkey, T.D. (1992) Theoretical considerations when estimating the mesophyll conductance to CO_2 flux by analysis of the response of photosynthesis to CO_2. *Plant Physiology*, 98, 1429–1436.

Harley, P.C. & Sharkey, T.D. (1991) An improved model of C_3 photosynthesis at high CO_2: reversed O_2 sensitivity explained by lack of glycerate reentry into the chloroplast. *Photosynthesis Research*, 27, 169–178.

Haworth, M., Marino, G. & Centritto, M. (2018) An introductory guide to gas exchange analysis of photosynthesis and its application to plant phenotyping and precision irrigation to enhance water use efficiency. *Journal of Water and Climate Change*, 9, 786–808.

Hermida-Carrera, C., Kapralov, M.V. & Galmés, J. (2016) Rubisco catalytic properties and temperature response in crops. *Plant Physiology*, 171, 2549–2561.

Hirasawa, T. & Hsiao, T.C. (1999) Some characteristics of reduced leaf photosynthesis at midday in maize growing in the field. *Field Crops Research*, 62, 53–62.

Hogewoning, S.W., van den Boogaart, S.A.J., van Tongerlo, E. & Trouwborst, G. (2021) CAM-physiology and carbon gain of the orchid *Phalaenopsis* in response to light intensity, light integral and CO_2. *Plant, Cell & Environment*, 44, 762–774.

Iñiguez, C., Niinemets, Ü., Mark, K. & Galmés, J. (2021) Analyzing the causes of method-to-method variability among Rubisco kinetic traits: from the first to the current measurements. *Journal of Experimental Botany*, 72, 7846–7862.

Johnson, J.E. & Berry, J.A. (2021) The role of Cytochrome b_6f in the control of steady-state photosynthesis: a conceptual and quantitative model. *Photosynthesis Research*, 148, 101–136.

Kitao, M., Harayama, H. & Uemura, A. (2017) A practical approach to estimate diffusional leakages of leaf chamber of open gas exchange systems using intact leaves. *Plant, Cell & Environment*, 40, 2870–2874.

Koester, R.P., Nohl, B.M., Diers, B.W. & Ainsworth, E.A. (2016) Has photosynthetic capacity increased with 80 years of soybean breeding? An examination of historical soybean cultivars. *Plant, Cell & Environment*, 39, 1058–1067.

Kromdijk, J. & Long, S.P. (2016) One crop breeding cycle from starvation? How engineering crop photosynthesis for rising CO_2 and temperature could be one important route to alleviation. *Proceedings of the Royal Society B: Biological Sciences*, 283, 20152578.

Laing, W.A., Ogren, W.L. & Hageman, R.H. (1974) Regulation of soybean net photosynthetic CO_2 fixation by the interaction of CO_2, O_2, and ribulose 1,5-diphosphate carboxylase. *Plant Physiology*, 54, 678–685.

Leakey, A.D., Bernacchi, C.J., Ort, D.R. & Long, S.P. (2006) Long-term growth of soybean at elevated [CO_2] does not cause acclimation of stomatal conductance under fully open-air conditions. *Plant, Cell & Environment*, 29, 1794–1800.

Li, S., Moller, C.A., Mitchell, N.G., Lee, D. & Ainsworth, E.A. (2021) Bioenergy sorghum maintains photosynthetic capacity in elevated ozone concentrations. *Plant, Cell & Environment*, 44, 729–746.

LI-COR. (2012) *Using the LI-6400/LI-6400XT portable photosynthesis system, version 6*. Lincoln, NE, USA: LI-COR Biosciences. https://www.licor.com/env/support/LI-6400/manuals.html

LI-COR. (2022) *Using the LI-6800 portable photosynthesis system, Bluestem OS v2.1*. Lincoln, NE, USA: LI-COR Biosciences. https://www.licor.com/env/support/LI-6800/manuals.html

de Lobo, F.A., de Barros, M.P., Dalmagro, H.J., Dalmolin, Â.C., Pereira, W.E., de Souza, É.C. et al. (2013) Fitting net photosynthetic light-response curves with Microsoft Excel — a critical look at the models. *Photosynthetica*, 51, 445–456.

Long, S.P. (2003) Gas exchange measurements, what can they tell us about the underlying limitations to photosynthesis? Procedures and sources of error. *Journal of Experimental Botany*, 54, 2393–2401.

Long, S.P., Farage, P.K. & Garcia, R.L. (1996) Measurement of leaf and canopy photosynthetic CO_2 exchange in the field. *Journal of Experimental Botany*, 47, 1629–1642.

Long, S.P. & Hallgren, J.E. (1985) Measurement of CO_2 assimilation by plants in the field and the laboratory. In: Coombs, J., Hall, D.O., Long, S.P. & Scurlock, J.M.O. (Eds.) *Techniques in bioproductivity and photosynthesis*. Oxford, UK: Pergamon Press Ltd., pp. 62–94.

Long, S.P. & Hällgren, J.-E. (1993) Measurement of CO_2 assimilation by plants in the field and the laboratory. In: Hall, D.O., Scurlock, J.M.O., Bolhàr-Nordenkampf, H.R., Leegood, R.C. & Long, S.P. (Eds.) *Photosynthesis and production in a changing environment: a field and laboratory manual*. Dordrecht: Springer Netherlands, pp. 129–167.

Lundgren, M.R., Christin, P.-A., Escobar, E.G., Ripley, B.S., Besnard, G., Long, C.M. et al. (2016) Evolutionary implications of C_3–C_4

intermediates in the grass *Alloteropsis semialata*. *Plant, Cell & Environment*, 39, 1874–1885.

Márquez, D.A., Stuart-Williams, H. & Farquhar, G.D. (2021) An improved theory for calculating leaf gas exchange more precisely accounting for small fluxes. *Nature Plants*, 7, 317–326.

Márquez, D.A., Stuart-Williams, H., Farquhar, G.D. & Busch, F.A. (2022) Cuticular conductance of adaxial and abaxial leaf surfaces and its relation to minimum leaf surface conductance. *New Phytologist*, 233, 156–168.

Matthews, J.S.A., Vialet-Chabrand, S. & Lawson, T. (2018) Acclimation to fluctuating light impacts the rapidity of response and diurnal rhythm of stomatal conductance. *Plant Physiology*, 176, 1939–1951.

Medlyn, B.E., Badeck, F.-W., De Pury, D.G.G., Barton, C.V.M., Broadmeadow, M., Ceulemans, R. et al. (1999) Effects of elevated [CO_2] on photosynthesis in European forest species: a meta-analysis of model parameters. *Plant, Cell & Environment*, 22, 1475–1495.

Medlyn, B.E., Dreyer, E., Ellsworth, D., Forstreuter, M., Harley, P.C., Kirschbaum, M.U.F. et al. (2002) Temperature response of parameters of a biochemically based model of photosynthesis. II. A review of experimental data. *Plant, Cell & Environment*, 25, 1167–1179.

Miner, G.L., Bauerle, W.L. & Baldocchi, D.D. (2017) Estimating the sensitivity of stomatal conductance to photosynthesis: a review. *Plant, Cell & Environment*, 40, 1214–1238.

Mott, K.A. & Buckley, T.N. (2000) Patchy stomatal conductance: emergent collective behaviour of stomata. *Trends in Plant Science*, 5, 258–262.

Mott, K.A. & Peak, D. (2011) Alternative perspective on the control of transpiration by radiation. *Proceedings of the National Academy of Sciences of the United States of America*, 108, 19820–19823.

Ögren, E. & Evans, J.R. (1993) Photosynthetic light-response curves. *Planta*, 189, 182–190.

Ögren, E. & Rosenqvist, E. (1992) On the significance of photoinhibition of photosynthesis in the field and its generality among species. *Photosynthesis Research*, 33, 63–71.

Orr, D., Alcântara, A., Kapralov, M.V., Andralojc, J., Carmo-Silva, E. & Parry, M.A.J. (2016) Surveying Rubisco diversity and temperature response to improve crop photosynthetic efficiency. *Plant Physiology*, 172, 707–717.

Panda, D. (2011) Diurnal variations in gas exchange and chlorophyll fluorescence in rice leaves: the cause for midday depression in CO2 photosynthetic rate. *Journal of Stress Physiology & Biochemistry*, 7, 175–186.

Parsons, R., Weyers, J.D.B., Lawson, T. & Godber, I.M. (1997) Rapid and straightforward estimates of photosynthetic characteristics using a portable gas exchange system. *Photosynthetica*, 34, 265–279.

Peak, D., Hogan, M.T. & Mott, K.A. (2023) Stomatal patchiness and cellular computing. *Proceedings of the National Academy of Sciences*, 120, e2220270120.

Pons, T.L., Flexas, J., von Caemmerer, S., Evans, J.R., Genty, B., Ribas-Carbo, M. et al. (2009) Estimating mesophyll conductance to CO_2: methodology, potential errors, and recommendations. *Journal of Experimental Botany*, 60, 2217–2234.

Poorter, H., Knopf, O., Wright, I.J., Temme, A.A., Hogewoning, S.W., Graf, A. et al. (2022) A meta-analysis of responses of C_3 plants to atmospheric CO_2: dose-response curves for 85 traits ranging from the molecular to the whole plant level. *New Phytologist*, 233, 1560–1596.

Prioul, J.L. & Chartier, P. (1977) Partitioning of transfer and carboxylation components of intracellular resistance to photosynthetic CO_2 fixation: a critical analysis of the methods used. *Annals of Botany*, 41, 789–800.

Rabinowitch, E.I. (1951) Photosynthesis and related processes *(vol. II part 1)*. New York, USA: Interscience Publishers Inc.

Rogers, A. (2014) The use and misuse of $V_{c,max}$ in earth system models. *Photosynthesis Research*, 119, 15–29.

Rogers, A., Medlyn, B.E. & Dukes, J.S. (2014) Improving representation of photosynthesis in earth system models. *New Phytologist*, 204, 12–14.

Rogers, A., Medlyn, B.E., Dukes, J.S., Bonan, G., von Caemmerer, S., Dietze, M.C. et al. (2017) A roadmap for improving the representation of photosynthesis in earth system models. *New Phytologist*, 213, 22–42.

Rogers, A., Serbin, S.P., Ely, K.S. & Wullschleger, S.D. (2019) Terrestrial biosphere models may overestimate arctic CO_2 assimilation if they do not account for decreased quantum yield and convexity at low temperature. *New Phytologist*, 223, 167–179.

Sage, R.F. & Kubien, D.S. (2007) The temperature response of C_3 and C_4 photosynthesis. *Plant, Cell & Environment*, 30, 1086–1106.

Sander, R. (2015) Compilation of Henry's law constants (version 4.0) for water as solvent. *Atmospheric Chemistry and Physics*, 15, 4399–4981.

Savvides, A.M. & Fotopoulos, V. (2018) Two inexpensive and non-destructive techniques to correct for smaller-than-gasket leaf area in gas exchange measurements. *Frontiers in Plant Science*, 9, 9.

Schindelin, J., Arganda-Carreras, I., Frise, E., Kaynig, V., Longair, M., Pietzsch, T. et al. (2012) Fiji: an open-source platform for biological-image analysis. *Nature Methods*, 9, 676–682.

Schuster, W.S. & Monson, R.K. (1990) An examination of the advantages of C_3-C_4 intermediate photosynthesis in warm environments. *Plant, Cell & Environment*, 13, 903–912.

Sharkey, T.D. (2016) What gas exchange data can tell us about photosynthesis. *Plant, Cell & Environment*, 39, 1161–1163.

Sharkey, T.D., Bernacchi, C.J., Farquhar, G.D. & Singsaas, E.L. (2007) Fitting photosynthetic carbon dioxide response curves for C_3 leaves. *Plant, Cell & Environment*, 30, 1035–1040.

Sharwood, R.E., Ghannoum, O., Kapralov, M.V., Gunn, L.H. & Whitney, S.M. (2016) Temperature responses of Rubisco from Paniceae grasses provide opportunities for improving C_3 photosynthesis. *Nature Plants*, 2, 16186.

Slot, M. & Winter, K. (2017) In situ temperature relationships of biochemical and stomatal controls of photosynthesis in four lowland tropical tree species. *Plant, Cell & Environment*, 40, 3055–3068.

Smith, E.L. (1937) The influence of light and carbon dioxide on photosynthesis. *Journal of General Physiology*, 20, 807–830.

Smith, H.L., McAusland, L. & Murchie, E.H. (2017) Don't ignore the green light: exploring diverse roles in plant processes. *Journal of Experimental Botany*, 68, 2099–2110.

Stinziano, J.R., Roback, C., Sargent, D., Murphy, B.K., Hudson, P.J. & Muir, C.D. (2021) Principles of resilient coding for plant ecophysiologists. *AoB Plants*, 13, plab059.

Sun, Y.R., Ma, W.T., Xu, Y.N., Wang, X., Li, L., Tcherkez, G. et al. (2023) Short- and long-term responses of leaf day respiration to elevated atmospheric CO_2. *Plant Physiology*, 191, 2204–2217.

Tcherkez, G., Gauthier, P., Buckley, T.N., Busch, F.A., Barbour, M.M., Bruhn, D. et al. (2017a) Leaf day respiration: low CO_2 flux but high significance for metabolism and carbon balance. *New Phytologist*, 216, 986–1001.

Tcherkez, G., Gauthier, P., Buckley, T.N., Busch, F.A., Barbour, M.M., Bruhn, D. et al. (2017b) Tracking the origins of the Kok effect, 70 years after its discovery. *New Phytologist*, 214, 506–510.

Tholen, D., Ethier, G., Genty, B., Pepin, S. & Zhu, X.-G. (2012) Variable mesophyll conductance revisited: theoretical background and experimental implications. *Plant, Cell & Environment*, 35, 2087–2103.

Thornley, J.H. (1976) *Mathematical models in plant physiology*. London: Academic Press (Inc.) Ltd.

Vialet-Chabrand, S., Matthews, J.S.A. & Lawson, T. (2021) Light, power, action! Interaction of respiratory energy- and blue light-induced stomatal movements. *New Phytologist*, 231, 2231–2246.

Walker, A.P., Beckerman, A.P., Gu, L., Kattge, J., Cernusak, L.A., Domingues, T.F. et al. (2014) The relationship of leaf photosynthetic traits – V_{cmax} and J_{max} – to leaf nitrogen, leaf phosphorus, and

specific leaf area: a meta-analysis and modeling study. *Ecology and Evolution*, 4, 3218–3235.

Walz. (2019) *Portable gas exchange fluorescence system GFS-3000: handbook of operation*, 9th edition, Effeltrich: Heinz Walz GmbH. https://www.walz.com/products/gas_exchange/gfs-3000/downloads.html

Weiss, I., Mizrahi, Y. & Raveh, E. (2009) Chamber response time: a neglected issue in gas exchange measurements. *Photosynthetica*, 47, 121–124.

Wittig, V.E., Ainsworth, E.A. & Long, S.P. (2007) To what extent do current and projected increases in surface ozone affect photosynthesis and stomatal conductance of trees? A meta-analytic review of the last 3 decades of experiments. *Plant, Cell & Environment*, 30, 1150–1162.

Wohlfahrt, G., Bahn, M., Haubner, E., Horak, I., Michaeler, W., Rottmar, K. et al. (1999) Inter-specific variation of the biochemical limitation to photosynthesis and related leaf traits of 30 species from mountain grassland ecosystems under different land use. *Plant, Cell & Environment*, 22, 1281–1296.

Wolz, K.J., Wertin, T.M., Abordo, M., Wang, D. & Leakey, A.D.B. (2017) Diversity in stomatal function is integral to modelling plant carbon and water fluxes. *Nature Ecology & Evolution*, 1, 1292–1298.

Wong, S.C., Canny, M.J., Holloway-Phillips, M., Stuart-Williams, H., Cernusak, L.A., Márquez, D.A. et al. (2022) Humidity gradients in the air spaces of leaves. *Nature Plants*, 8, 971–978.

Yamori, W., Hikosaka, K. & Way, D.A. (2014) Temperature response of photosynthesis in C_3, C_4, and CAM plants: temperature acclimation and temperature adaptation. *Photosynthesis Research*, 119, 101–117.

Yan, W., Zhong, Y. & Shangguan, Z. (2016) A meta-analysis of leaf gas exchange and water status responses to drought. *Scientific Reports*, 6, 20917.

Yin, X., Busch, F.A., Struik, P.C. & Sharkey, T.D. (2021) Evolution of a biochemical model of steady-state photosynthesis. *Plant, Cell & Environment*, 44, 2811–2837.

Yin, X. & Struik, P.C. (2009) Theoretical reconsiderations when estimating the mesophyll conductance to CO_2 diffusion in leaves of C_3 plants by analysis of combined gas exchange and chlorophyll fluorescence measurements. *Plant, Cell & Environment*, 32, 1513–1524.

Zhen, S. & Bugbee, B. (2020) Far-red photons have equivalent efficiency to traditional photosynthetic photons: implications for re-defining photosynthetically active radiation. *Plant, Cell & Environment*, 43, 1259–1272.

SUPPORTING INFORMATION

Additional supporting information can be found online in the Supporting Information section at the end of this article.